10.6 Micron Parametric Frequency Converter

Hughes Research Laboratories

May 30, 1976

10.6 MICRON PARAMETRIC FREQUENCY CONVERTER

C.K. Asawa, T.K. Plant, and R.L. Abrams

Hughes Research Laboratories
3011 Malibu Canyon Road
Malibu, CA 90265

30 May 1976

Contract N00014-75-C-0089, Mod. P00002
Semiannual Technical Report 3
For Period 1 November 1975 Through 30 April 1976

Sponsored By
DEFENSE ADVANCED RESEARCH PROJECTS AGENCY
ARPA Order No. 1806

Monitored By
OFFICE OF NAVAL RESEARCH
800 North Quincy Street
Arlington, VA 22217

DISCLAIMER NOTICE

THIS DOCUMENT IS THE BEST QUALITY AVAILABLE.

COPY FURNISHED CONTAINED A SIGNIFICANT NUMBER OF PAGES WHICH DO NOT REPRODUCE LEGIBLY.

ARPA Order No.	1806
Program Code Number	5E20
Effective Date of Contract	1 September 1974
Contract Expiration Date	31 October 1976
Amount of Contract	$174,956.00
Principal Investigator	R.L. Abrams (213) 456-6411, Ext. 498
Scientific Officer	Director, Physics Program Physical Sciences Division Office of Naval Research 800 North Quincy Street Arlington, Virginia 22217

This research was supported by the Advanced Research Projects Agency of the Department of Defense and was monitored by ONR under Contract No. N00014-75-C-0089, Mod. P00002.

Unclassified

SECURITY CLASSIFICATION OF THIS PAGE (When Data Entered)

REPORT DOCUMENTATION PAGE	READ INSTRUCTIONS BEFORE COMPLETING FORM
1. REPORT NUMBER / 2. GOVT ACCESSION NO	3. RECIPIENT'S CATALOG NUMBER
4. TITLE (and Subtitle) 10.6 Micron Parametric Frequency Converter	5. TYPE OF REPORT & PERIOD COVERED Semiannual Tech Report 3 1 Nov 1975 – 30 Apr 1976 6. PERFORMING ORG. REPORT NUMBER
7. AUTHOR(s) C.K. Asawa, T.K. Plant and R.L. Abrams	8. CONTRACT OR GRANT NUMBER(s) N00014-75-C-0089 Mod. P00002
9. PERFORMING ORGANIZATION NAME AND ADDRESS Hughes Research Laboratories 3011 Malibu Canyon Road Malibu, California 90265	10. PROGRAM ELEMENT, PROJECT, TASK AREA & WORK UNIT NUMBERS ARPA Order No. 1806 Program Code No. 5E20
11. CONTROLLING OFFICE NAME AND ADDRESS Defense Advanced Research Projects Agency 1400 Wilson Boulevard Arlington, Virginia 22209	12. REPORT DATE May 1976 13. NUMBER OF PAGES 77
14. MONITORING AGENCY NAME & ADDRESS (if different from Controlling Office) Office of Naval Research 800 No. Quincy Street Arlington, Virginia 22217	15. SECURITY CLASS. (of this report) Unclassified 15a. DECLASSIFICATION/DOWNGRADING SCHEDULE

16. DISTRIBUTION STATEMENT (of this Report)

Approved for public release; distribution unlimited.

17. DISTRIBUTION STATEMENT (of the abstract entered in Block 20, if different from Report)

18. SUPPLEMENTARY NOTES

19. KEY WORDS (Continue on reverse side if necessary and identify by block number)

CO_2 Laser
Nonlinear Mixing
Frequency Conversion
Tunable Laser

20. ABSTRACT (Continue on reverse side if necessary and identify by block number)

The first observation of resonantly-enhanced Stark-induced two-photon mixing in a gas was previously reported on this program. Parametric single sideband generation in $N^{14}H_2D$ at the difference frequency of 10.6 μm and 4 GHz microwave radiation was described. During this reporting period, exact confirmation of the theoretical prediction of conversion efficiency versus gas pressure was established by new precision measurements of the $N^{14}H_2D$ absorption linewidth versus pressure.

DD FORM 1 JAN 73 1473 EDITION OF 1 NOV 65 IS OBSOLETE

Unclassified

SECURITY CLASSIFICATION OF THIS PAGE (When Data Entered)

Output parametric conversion efficiency of 0.2% was measured with a new ridged waveguide; no evidence of microwave power saturation was observed.

Two new parametric converter systems that promise increased parametric gain and conversion efficiency (several times to two orders of magnitude) have been identified. These are: (1) the $C^{12}O_2^{16}$ P(24) laser line and 2.15 GHz microwave radiation resonating with the Stark tuned vibrational-rotational transitions of $N^{15}H_2D$ and (2) the isotopic $C^{13}O_2^{16}$ R(18) laser line and 26.378 GHz microwave radiation resonating with $N^{14}H_3$. The basis for the increased gain is described. Construction of suitable microwave Stark cells for these two systems is underway.

Previous theoretical and experimental results are included as appendices.

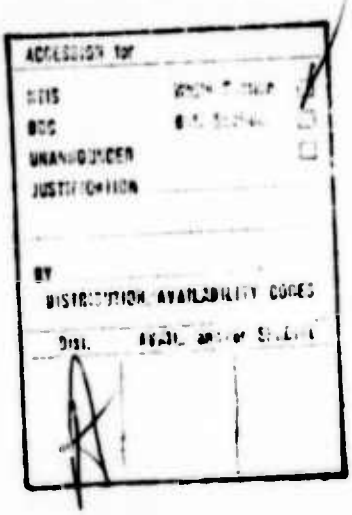

TABLE OF CONTENTS

LIST OF ILLUSTRATIONS

PREFACE

The following personnel contributed to the research reported here: C. K. Asawa, T. K. Plant, G. L. Tangonan and F. L. Abrams. Technical assistance was provided by R. E. Brower.

I. INTRODUCTION AND SUMMARY

A. Background

We anticipate that modern optical radar systems for surveillance of orbiting objects will require new types of electro-optical devices capable of frequency control and frequency conversion of infrared (IR) laser radiation. This program addresses an approach that should lead to a new class of electro-optical devices such as single sideband modulators, tunable local oscillators, and frequency shifters, using the resonant interaction of optical and microwave fields in a gas whose energy level structure is controlled by an applied electric field (Stark effect).

We have demonstrated on this program, both theoretically and experimentally, that single sideband generation is indeed possible by mixing laser and microwave radiation in a Stark-induced nonlinear gas. The initial experiments were performed with the $C^{12}O_2^{16}$ P(20) laser line at 10.6 μm and 4 GHz microwave mixed in a microwave Stark cell containing $N^{14}H_2D$, resulting in a resonantly enhanced output at the lower sideband near 10.6 μm. These experiments have shown that, with suitable Stark molecules, new spectrally down-converted or up-converted optical frequencies are now available for the application cited above.

B. Basic Concept

To illustrate the basic mechanism for the interaction, consider the simplified energy level diagram of NH_2D shown in Fig. 1. Upon application of an electric field of appropriate magnitude, two NH_2D energy levels, labeled 1 and 3 in Fig. 1, will become resonant with the laser frequency. A third level (level 2) is also tuned by the electric field. The key element of this system is that the applied field breaks inversion symmetry and induces a permanent dipole moment. The three electric dipole moments μ_{12}, μ_{13}, μ_{23} are all nonzero, due to the applied electric field, and this allows us to consider a number of

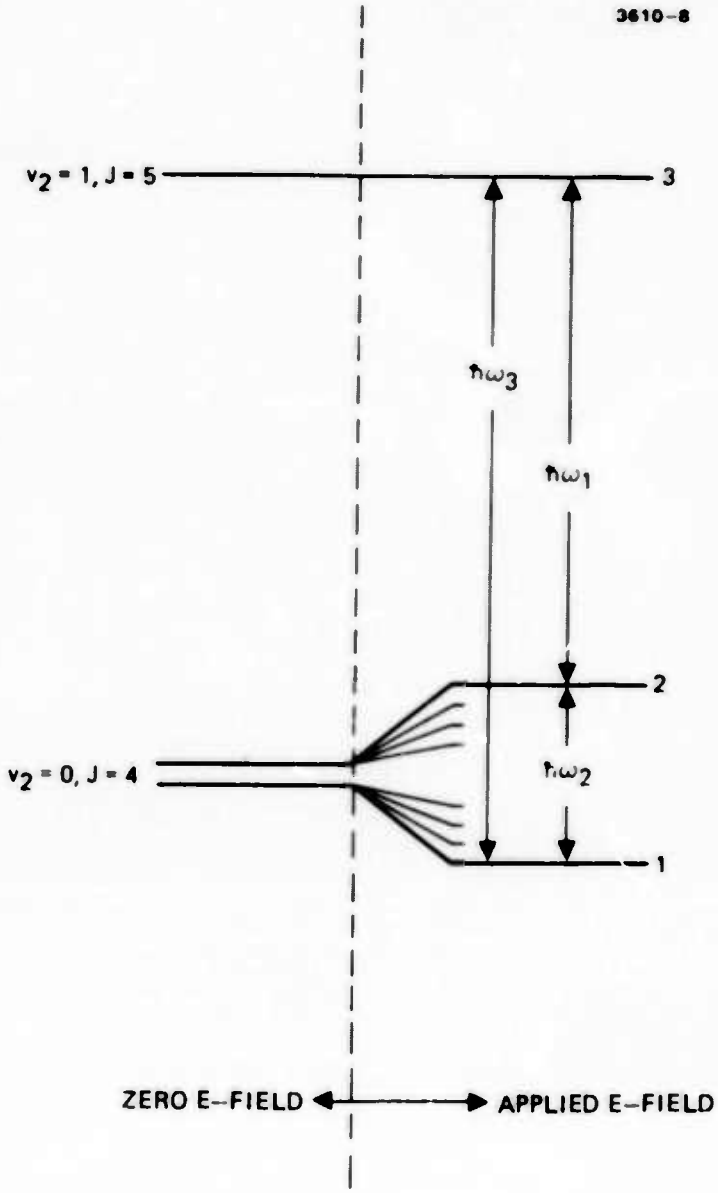

Fig. 1.
Simplified energy level diagram for $^{14}NH_2D$, showing relevant levels in an applied electric field. The P(20) 10.6 μm radiation is incident at frequency ω_3, ω_2 is the applied microwave frequency, and ω_1 is the newly generated sideband frequency.

possible strong interactions which would ordinarily be weak. The experiment involves the simultaneous application of two fields to the NH_2D: an applied field at ω_2 resonant with levels 1 and 2 at the microwave frequency, and a field at ω_3 resonant with levels 1 and 3 at 10.6 μm. Resonantly enhanced nonlinear mixing in the NH_2D gas results in the generation of a signal at $\omega_1 = \omega_3 - \omega_2$ with measureable conversion efficiencies. A complete description is given in the Appendices. A theoretical description of this process is summarized in Appendix A. The first observation of parametric generation in a Stark gas is summarized in Appendix B.

C. Progress

During this reporting period exact confirmation of the theoretical prediction of parametric conversion efficiency versus gas pressure was established by new precision measurements of the $N^{14}H_2D$ absorption linewidth versus pressure. Previous published data on the high pressure absorption coefficient and the pressure broadening coefficient were found to be in error. By fitting absorption curves versus Stark voltage at various pressures to a Voigt profile, the homogeneous linewidth pressure broadening coefficient, Γ, of 40.2 ± 0.4 MHz/Torr (FWHM) was extracted, which is considerably different than published data of 64 MHz/Torr (used earlier in evaluating our parametric results). We found the high pressure absorption coefficient γ_H to be 0.028 cm^{-1} in contrast to the published value of 0.042 cm^{-1}.

Using the new values of γ_H and Γ, an excellent fit of the theoretically derived parametric signal variation versus pressure with the experimental curve was obtained requiring no scaling of the abscissa.

A new ridged waveguide cavity incorporating a number of improvements over the original cavity was constructed. The end gap of the original cavity was eliminated; matched coupling to the cavity was more readily attained with a new short round bead located closer to the ridge of the cavity. Parametric conversion efficiency of 0.2% was attained with the new cavity at a pressure of 2.2 Torr.

Two new parametric converter systems promising increased conversion gains and efficiencies have been identified. These are:

(1) The $C^{12}O_2^{16}$ P(26) laser line and the rotational-vibrational lines of $N^{15}H_2D$. The microwave resonance frequency is 2.15 GHz.

(2) The isotopic $C^{13}O_2^{16}$ R(18) line at 10.784 μm resonating with the asQ(6, 6, 6) transition of $N^{14}H_3$. The microwave frequency is increased to 26.378 GHz, the transition occurrring between Stark split inversion levels. The parametric output is upconverted for this system (sum frequency) in contrast to down conversion in system (1) and the original $C^{12}O_2^{16}$ P(20), $N^{14}H_2D$ system.

The conversion efficiencies of systems (1) and (2) with respect to the original system are calculated to be 3.2 and 121, respectively. A technique for making these projections is described.

The test microwave Stark cavity for 26 GHz has been constructed. Due to more stringent requirements on phase matching at 26 GHz, the laser beam will be propagated at $\sim 30^{\circ}$ to the cavity axis in the test cavity.

D. Plans

During the final half year of the program the emphasis will be on constructing new cavities and testing the two promising new systems, ($C^{12}O_2^{16}$ P(26), $N^{15}H_2D$) and ($C^{13}O_2^{16}$ R(18), $N^{14}H_3$), with a goal towards gaining conversion efficiencies approaching 10%. The effect of molecular absorption of the laser beam on the parametric process will be examined in greater detail; an analysis of the effect of high absorption on conversion efficiency is presently underway.

II. THEORETICAL AND EXPERIMENTAL PROGRESS

A detailed description of the progress during the last half year, as summarized in Section I-C, is included here.

A. Linewidth Measurement of $N^{14}H_2D$

In the last interim report the pressure variation of the parametric signal was discussed. It was shown that the theoretical pressure variation agreed well with the experimental results if the pressure abscissa was scaled by nearly a factor of two to match the points of maximum parametric signal for both curves. This scaling factor was ascribed to inhomogeneities in the Stark field. When careful alignment of the Stark field gap later failed to remove the discrepancy, we decided that our assumed values of the high pressure absorption coefficient γ_H and of the pressure broadening coefficient Γ might be in error.

To resolve this question, we performed a series of careful measurements of the $N^{14}H_2D$ $(0_a, 4_{04}, 4) \rightarrow 1_a, 5_{05}, 5)$ absorption versus Stark voltage for cell pressures from 0.50 to 10.0 Torr. By fitting these curves to Voigt profiles with a specified Doppler broadened halfwidth, the homogeneous linewidth pressure broadening coefficient was extracted. Since less than 0.5% variation in the Stark spacing results in a 4 MHz addition to the theoretical Doppler width of 82 MHz (FWHM), it was necessary to let the effective Doppler width vary from 82 MHz to 88 MHz and pick the best fit to the Voigt profile consistent with our measured low pressure linewidth.

The resulting pressure broadening coefficient Γ for our gas mixture ($N^{14}H_3$:$N^{14}D_3$ = 2:1) was 40.2 ± 0.4 MHz/Torr (FWHM) which was considerably different than the previously reported value of 64 MHz/Torr we used earlier. After correcting for $|M| = 3$ absorption at higher pressures, the variation of the $|M| = 4$ absorption coefficient versus

pressure was plotted as shown in Fig. 2. Here the dots are the data points and the solid curve is the theoretical line center absorption of the Voigt profile using 40.2 MHz/Torr as the broadening parameter. The high pressure absorption coefficient γ_H was found to be 0.028 cm^{-1}, again much different than the value of 0.042 cm^{-1} reported in the literature. The above results are described in further detail in Appendix C.

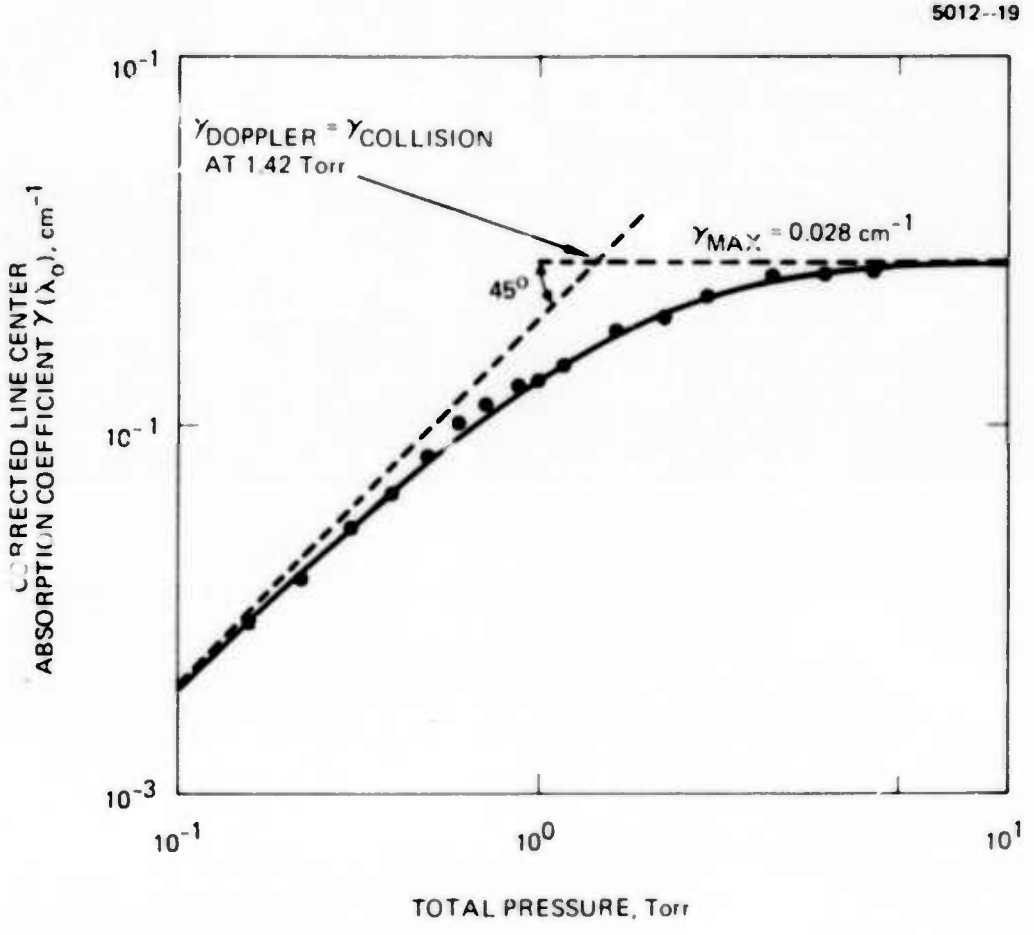

Fig. 2. Corrected line center absorption coefficient ($|M| = 3$ effects subtracted) versus Stark cell pressure, for the $C^{12}O_2^{16}$ P(20) laser line in $N^{14}H_2D$.

Using these new values for γ_H and Γ in the theoretical expression for the parametric signal variation with pressure yielded an excellent fit to the experimental curve with no scaling necessary for the abscissa. This is another satisfying confirmation of the theoretical model and is shown in Fig. 3.

B. Results for a New 4 GHz Stark-Microwave Cavity

A new Stark-microwave cavity was constructed as a result of the examination of the microwave characteristics of the old cavity. It was found that the resonant frequency of the old cavity was at 3.82 GHz and was not moved by a tuning stub in series with the cavity. Placing metal shims at the ends of the ridge to fill the gap between the ridge and the end of the cavity shifted the resonant frequency to 4.1 GHz but the parametric conversion efficiency remained at 0.5×10^{-3}.

The new cavity contains several new ideas. By lengthening it to 20.5 cm and widening the ridge to 0.80 cm, the resonant frequency should be 4.13 GHz and the impedance of the open-ridged waveguide dropped to 50 Ω. The ridge was made only 3 mils shorter than the outer cavity to minimize the end gap and, hopefully, increase the microwave continuity at the ends of the ridge. The cavity was made in only three pieces – a base, a top, and the ridge which is fastened to the base from below.

A second lid was made with a very weakly coupled probe directly over the ridge. Using this test lid, the relative field along the ridge was measured for different input coupling configurations. The best coupler found to date is a short (~ 1/8 in.) round bead inserted from the gap side of the cavity positioned at $\lambda_g/4$ from one end of the cavity, and as close to the ridge as possible without danger of arcing. This probe still exhibits ~45% power reflection at maximum microwave power input and is an area of ongoing effort for improvement.

From the frequency response of the ridge probe in the test lid, the Q of the cavity appears to be ~120 at a resonant frequency of 4.13 GHz. This Q value is a very sensitive function of the contact

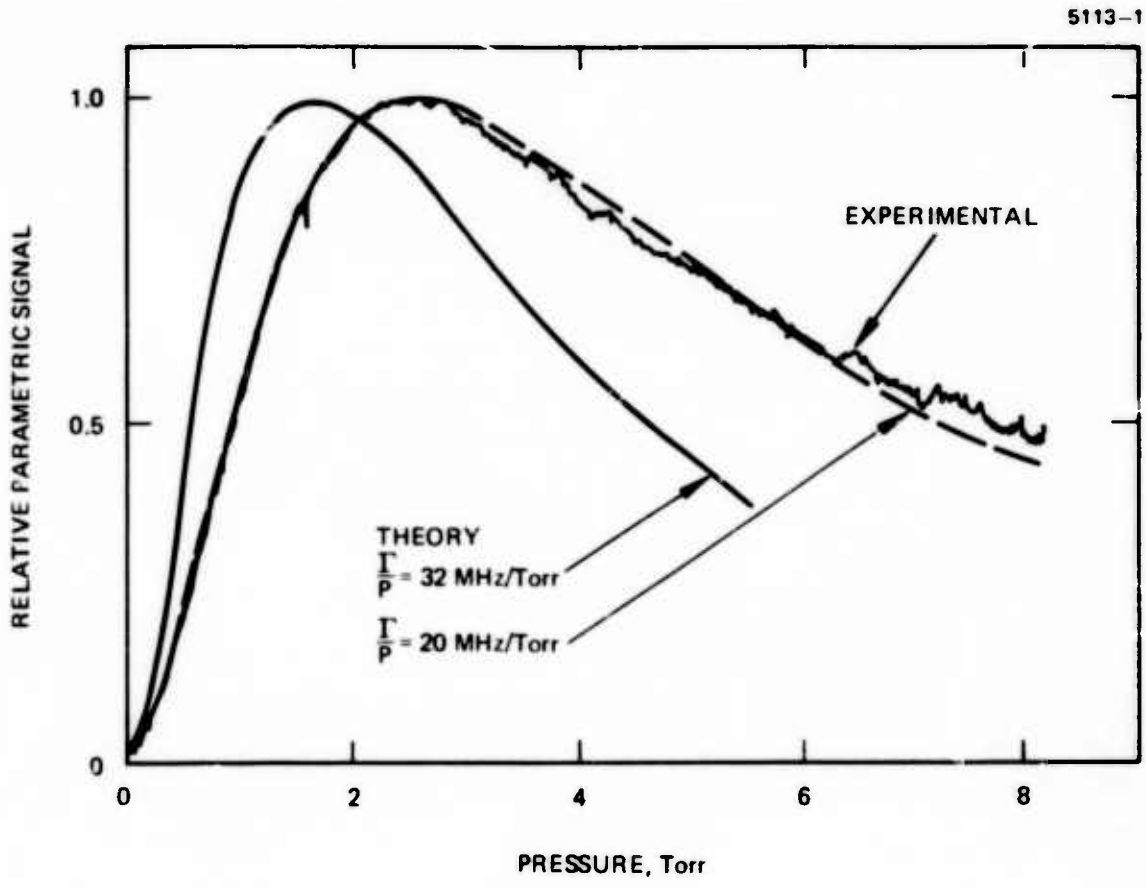

Fig. 3. Experimental plot of parametric signal versus cell pressure with theoretical prediction curves. Solid curve is for previous values of Γ and γH. Dashed curve is for new corrected values. Both curves unscaled in the abscissa.

between the lid and the cavity as evidenced by the large changes caused by tightening or loosening the lid screws slightly. Thus the cavity Q with the vacuum-sealed lid is not accurately known.

A series of standing wave ratio measurements have been made to measure the real cavity Q. However, the analysis of these data is complicated by the fact that the cavity resonance is not adjustable, making the detuned short position indeterminate. Work is still in progress to measure the cavity Q and also to measure the microwave resonance frequency when the Stark voltage is tuned to the CO_2 resonance absorption.

The CO_2 laser source was changed from a conventional laser to a Stark tunable waveguide laser to allow tuning the P(20) CO_2 laser frequency over a range of $\pm$ 300 MHz from line center. The nominal output of this laser is 250 mW. The rapidly diverging beam is nearly collimated with a lens and then masked with an iris to avoid reflected power effects.

New efficiency measurements were taken by setting the cavity pressure to the optimum 2.2 Torr and varying the laser frequency and Stark voltage for maximum parametric signal. The maximum conversion efficiency seen to date is 0.2%.

C. High Parametric Gain Potential with Two New Laser Lines and Molecular Systems

Two new laser lines and molecular systems with promising parametric conversion gains of 1.8 and 11 times that for the first parametric converter system ($C^{12}O_2^{16}$ P(20), $N^{14}H_2D$) have been identified. These are, respectively,

(1) The P(26) line of the $C^{12}O_2^{16}$ laser resonating with the isotopic $N^{15}H_2D$ molecule. The microwave frequency is 2.15 GHz.

(2) The R(18) line of the isotopic $C^{13}O_2^{16}$ laser resonating with the $N^{14}H_3$ molecule. The microwave frequency is 26.378 GHz.

The conversion efficiency (for small interaction distances) varies as the square of the gain, so that these two systems promise to show efficiencies 3.2 and 121 times greater than that of the initial system. Before describing the basis for this projection, the Stark absorption spectra of these two systems are shown.

1. Absorption Spectra for the Two New Systems

The Stark absorption spectrum of $N^{15}H_2D$ for the P(26) line of the $C^{12}O_2^{16}$ laser is shown in Fig. 4(a). A peak absorption of 14% for a 10-cm cell and 1-Torr pressure is shown. The absorption coefficient is 0.015 cm^{-1} $Torr^{-1}$. The Stark resonance voltage for the $|M| = 4$, $\Delta M = \pm 1$ transition is only 179 V over a 0.127 cm gap, the low voltage being an advantage with respect to electrical breakdown. Analysis of this transition in $N^{15}H_2D$ (Appendix D) shows that the states involved correspond precisely to the $N^{14}H_2D$ transition resonating with the P(20) line of the $C^{12}O_2^{16}$ laser (See Fig. 1, Appendix A). The zero field energy gap is 1.42 GHz for $N^{15}H_2D$, compared to 0.644 GHz for $N^{14}H_2D$.

The Stark absorption spectrum of $N^{14}H_3$ for the R(18) line of the isotopic $C^{13}O_2^{16}$ laser is shown in Fig. 4(b). Absorption of 100% for a 10-cm cell at 0.45 Torr pressure is shown. The absorption coefficient of the peak is 0.22 cm^{-1} $Torr^{-1}$, an exceptionally high value that should enhance parametric conversion. The energy levels of $N^{14}H_3$ and the transitions involved in parametric interactions are shown in Fig. 5. The Stark splitting involves the inversion-split levels of a single K level, not adjacent ($J_{K-1\,K-1}$) levels as for the asymmetric NH_2D molecule. The electric field is higher at 6452 V/cm for the $|M| = 6$ resonance. One notable feature of the $N^{14}H_3$ system is that the parametric output is up-converted to the sum frequency in contrast to down-conversion for the $N^{14}H_2D$ and $N^{15}H_2D$ systems. The upconverted output is suitably located in an atmospheric window.

5113-2

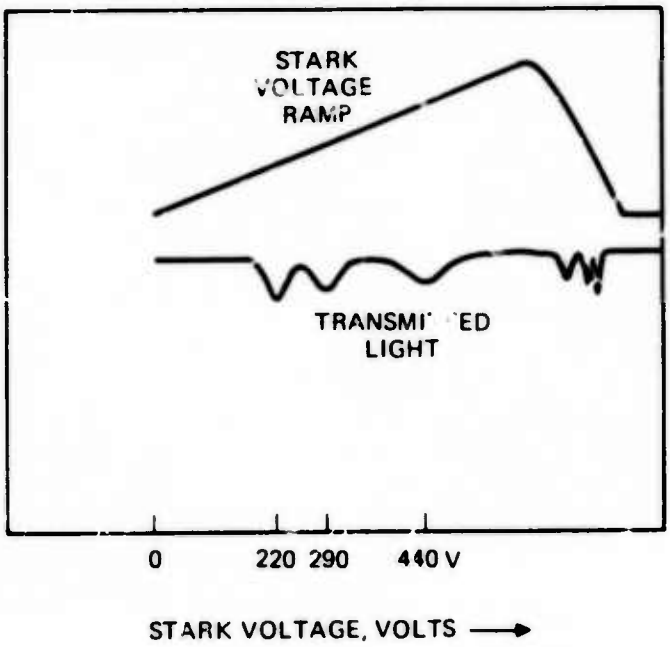

(a)

TRANSMISSION OF THE P (26) LINE OF THE $C^{12}O_2^{16}$ LASER THROUGH A STARK CELL CONTAINING $N^{15}H_2D$, AS A FUNCTION OF STARK VOLTAGE. PRESSURE 1.0 Torr. $N^{15}H_3 + D_2O$ MIXTURE. 14 % PEAK ABSORPTION IN 10 cm CELL' STARK GAP, 0.127 cm.

5113-3

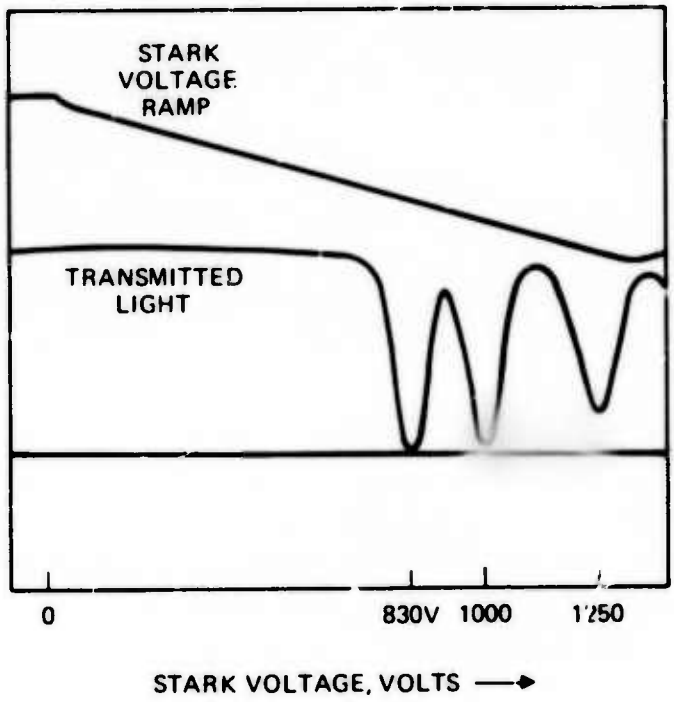

(b)

TRANSMISSION OF THE R(18) LINE OF THE ISOTOPIC $C^{13}O_2^{16}$ LASER THROUGH A STARK CELL CONTAINING $N^{14}H_3$, AS A FUNCTION OF STARK VOLTAGE. PRESSURE 0.450 Torr. 10 cm CELL. STARK GAP, 0.127 cm.

Fig. 4. Stark absorption spectra for two new laser lines and molecules. Parametric conversion efficiencies for the (a) and (b) systems are calculated to be 3 and 121 times that for the $C^{12}O_2^{16}$ P(20), $N^{14}H_2D$ system, respectively.

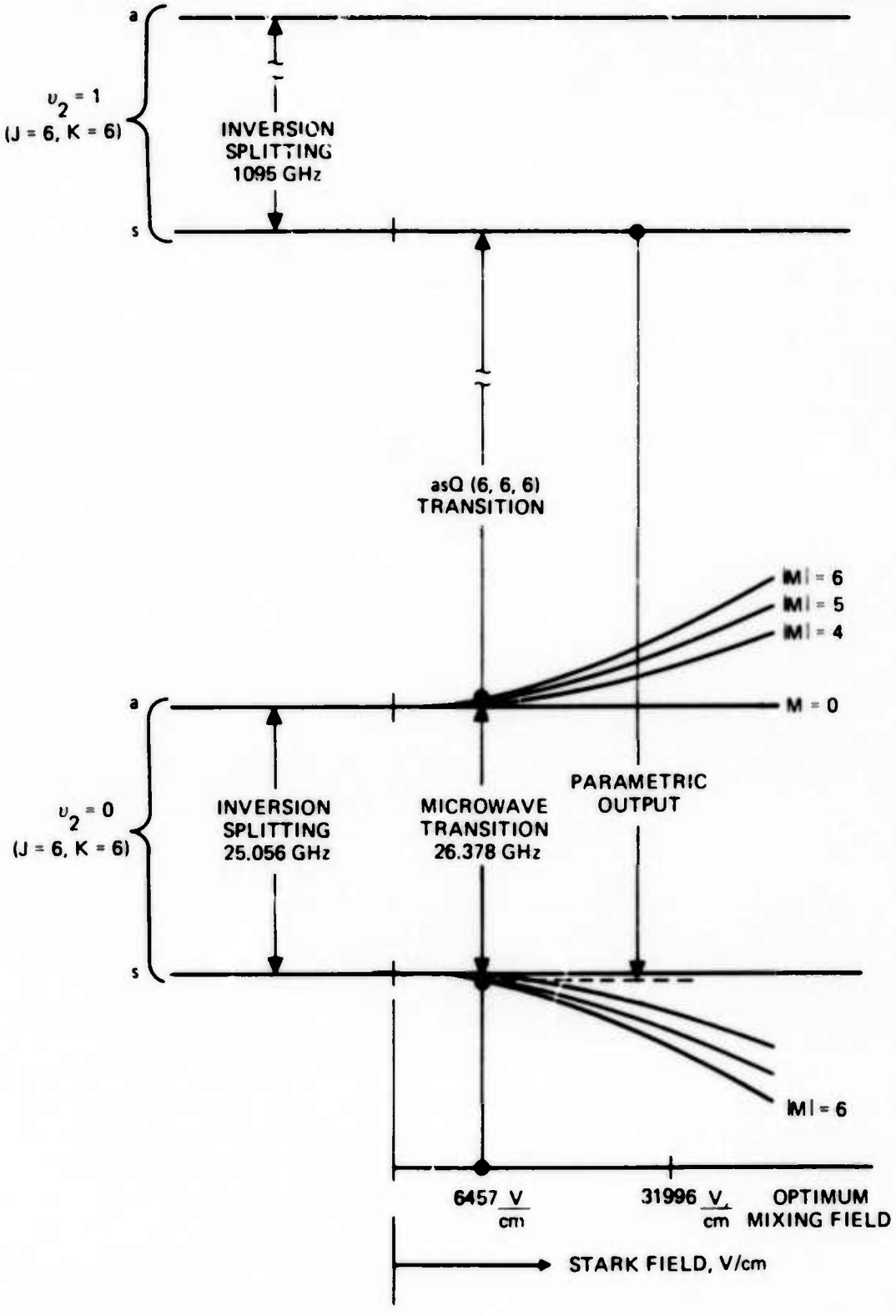

Fig. 5. Energy levels of $N^{14}H_3$ involved in the resonant parametric interaction. The $C^{13}O_2^{16}$ R(18) laser line is resonant with the asQ(6, 6, 6) transition. The parametric output is upconverted. The s→s transition is forbidden in this symmetric top with zero Stark field.

2. Parametric Gain as a Function of Stark Field Mixing of States

The model for the gain calculation is shown in Fig. 6. The zero field states are indicated by the subscript o. Assume that an electric dipole transition between one of the lower states $|2_o\rangle$ to the excited state $|3_o\rangle$ is forbidden with zero Stark field. The mixing of zero field states with the application of a Stark field permits transitions between all three perturbed states as indicated in Fig. 6. The perturbed states are written as linear combinations of the zero field states:

$$|1\rangle = b_1|1_o\rangle + b_2|2_o\rangle \ ,$$
$$|2\rangle = -b_2|1_o\rangle + b_1|2_o\rangle \ , \tag{1}$$

where b_1 and b_2 are the mixing coefficients

$$b_1 = \left[\frac{\sqrt{\delta^2+4E_{dc}^2\mu_{1_o2_o}^2} + \delta}{2\sqrt{\delta^2+4E_{dc}^2\mu_{1_o2_o}^2}}\right]^{1/2} \ ,$$
$$\tag{2}$$
$$b_2 = \left[\frac{\sqrt{\delta^2+4E_{dc}^2\mu_{1_o2_o}^2} - \delta}{2\sqrt{\delta^2+4E_{dc}^2\mu_{1_o2_o}^2}}\right]^{1/2} \ ,$$

and where

$\mu_{1_o2_o}$ = matrix element between zero field states $|1_o\rangle$ and $|2_o\rangle$

δ = zero field/splitting,

E_{dc} = Stark field.

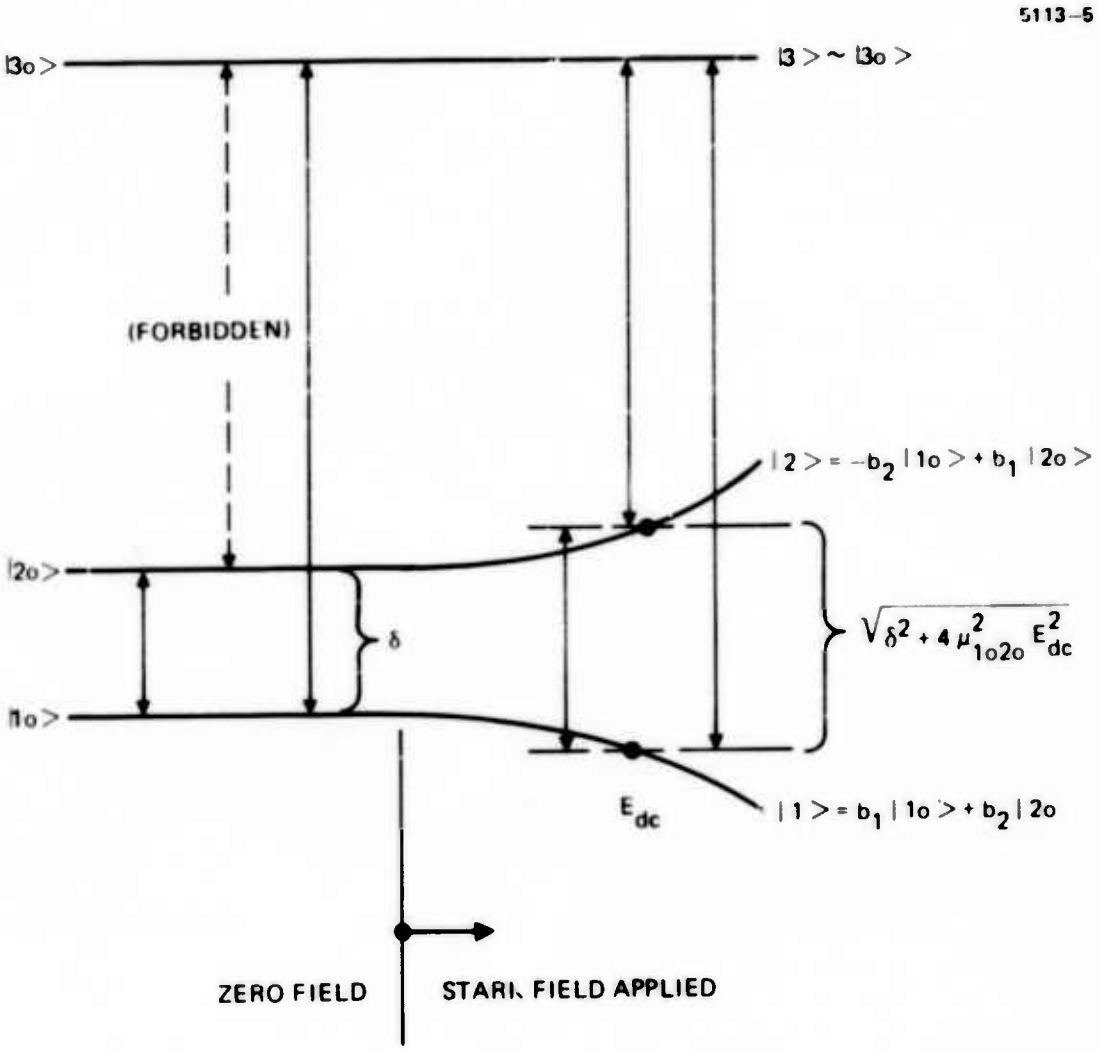

Fig. 6. General energy level diagram. Mixing of states by Stark field permit transitions between all three pairs of states. Optimum mixing for parametric conversion occurs when the two ground states are split by 1.27 δ, where δ is the zero field splitting.

An optimum Stark field mixing of the zero field states maximizes the parametric gain coefficient which depends explicity upon the mixing coefficients b_1 and b_2. The parametric gain coefficient g is proportional to

$$g \propto N_1 E_2 \mu_{12} \mu_{13} \mu_{32} \tag{3}$$

where

N_1 = population density of perturbed state $|1\rangle$

E_2 = microwave electric field (between levels $|1\rangle$ and $|2\rangle$)

μ_{ij} = electric dipole matrix element between perturbed states $|i\rangle$ and $|j\rangle$

From Fig. 6 it is readily seen that (3) can be written so that

$$g \propto -N_1 E_2 \mu_{1_o 2_o} \left(\mu_{1_o 3_o}\right)^2 \left(b_1^2 - b_2^2\right) b_1 b_2 \tag{4}$$

where the matrix elements are with respect to zero field states.

For evaluation purposes, rewrite g as

$$g \propto -N_1 E_2 \mu_{1_o 2_o} \left(b_1 \mu_{1_o 3_o}\right)^2 \left[\left(b_1^2 - b_2^2\right)\frac{b_2}{b_1}\right] \tag{5}$$

The $(b_1 \mu_{1_o 3_o})^2$ factor is proportional to the measured Stark absorption coefficient so that the measured values can be used for evaluating the gain for each system. The mixing coefficient to be optimized is then the factor in brackets, defined as g_o:

$$g_o \equiv \left(b_1^2 - b_2^2\right)\frac{b_2}{b_1} \tag{6}$$

Substituting (2) in (5),

$$g_o = \frac{\delta}{2E_{dc}\mu_{1_o 2_o}} \left[1 - \frac{1}{\sqrt{1 + \left(\frac{2E_{dc}\mu_{1_o 2_o}}{\delta} \right)^2}} \right]. \quad (7)$$

$g_o = 0$ for $E_{dc} = 0$ and infinity. A maximum value for g_o occurs at an intermediate value given by

$$2E_{dc\ opt}\mu_{1_o 2_o} = \left(\frac{1 + \sqrt{5}}{2} \right)^{1/2} \delta \quad . \quad (8)$$

$E_{dc\ opt}$ is the optimum Stark mixing field.

g_o can then be written as

$$g_o = \frac{1}{\left(\frac{1 + \sqrt{5}}{2} \right)^{1/2} \frac{E_{dc}}{E_{dc\ opt}}} \left[1 - \frac{1}{\sqrt{1 + \left(\frac{1 + \sqrt{5}}{2} \right) \frac{E_{dc}^2}{E_{dc\ opt}^2}}} \right]. \quad (9)$$

g_o is graphed as a function of $E_{dc}/E_{dc\ opt}$ in Fig. 7. The maximum value of g_o is 0.30, which occurs for a molecular system when the Stark field mixes the zero field states by an optimum amount.

3. Relative Parametric Gain for the Two New Systems

The relative parametric gains for the two new systems with respect to the original ($C^{12}O_2^{16}$ P(20), $N^{14}H_2D$) system are compared. g_o for the original system was 0.16 as indicated in Fig. 7; (6) shows that g_o depends upon the zero field splitting δ, the Stark field E_{dc}, and the dipole matrix element between the zero field states $|1_o\rangle$ and $|2_o\rangle$ and is a dimensionless factor.

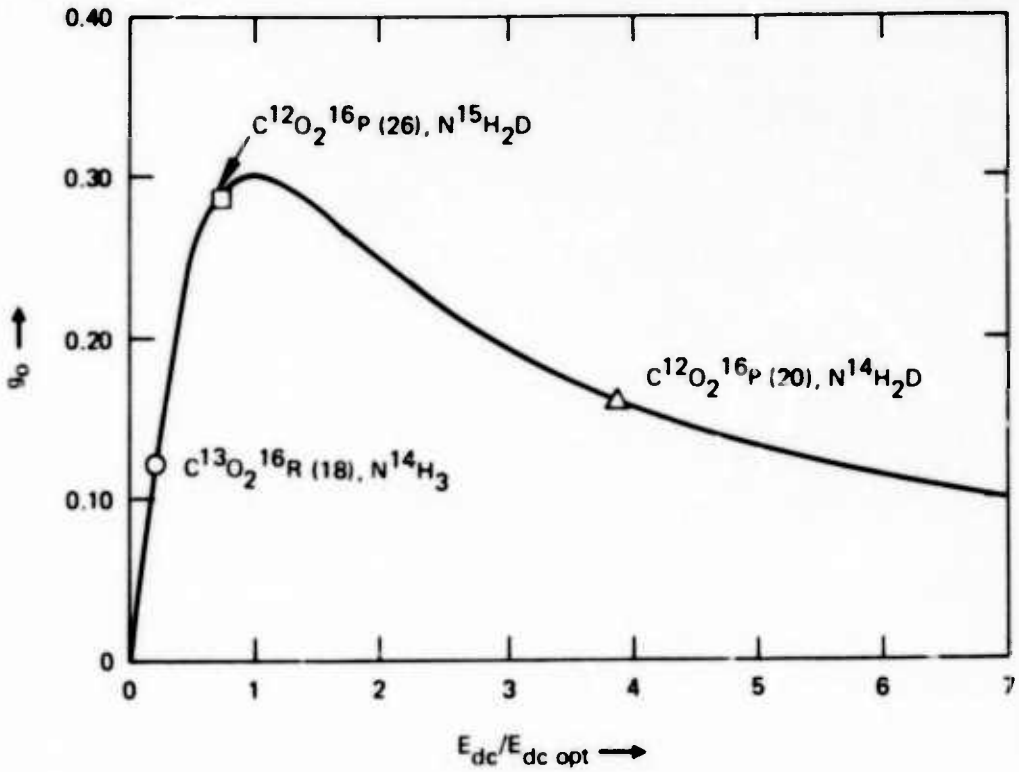

Fig. 7. Parametric conversion gain factor as function of Stark field. The optimum Stark field is that which splits the ground state to 1.618 times the zero field splitting. Parameters for the three systems are listed below:

△ = P(20) of $C^{12}O_2^{16}$ (10.6 μm) and $\nu_o = 0$, $4_{04} \rightarrow \nu_2 = 1$, 5_{05}, $\Delta M = +1$, transition of $N^{14}H_2D$, $\delta = 644$ MHz, $E_{opt} = 908$ V/cm, E = 3543 V/cm, $\mu = 1.14$ Debye, $\nu_{12} = 4.134$ GHz.

□ = P(26) of $C^{12}O_2^{16}$ (10.6 μm) and $\nu_o = 0$, $4_{04} \rightarrow \nu_2 = 1$, 5_{05}, transition of $N^{15}H_2D$, $\delta = 1420$ MHz, $E_{opt} = 2001$ V/cm, E = 1409 V/cm, $\mu = 1.14$ Debye, $\nu_{12} = 2.15$ GHz.

○ = R(18) of $C^{13}O_2^{16}$ (10.6 μm) and sQ(6.6) of N^4H_3, $\Delta M = 0$. $\delta = 25056$ MHz, $E_{opt} = 31996$ V/cm, E = 6452 V/cm, $\mu_{1o2o} = \mu(6/7)$, $\mu = 1.468$ Debye, $\nu_{12} = 26.378$ GHz.

g_o is 0.294, or near maximum, for the first new system ($C^{12}O_2^{16}$ P(26), $N^{15}H_2D$), as shown on Fig. 7. State mixing is near optimum. g is dependent upon the factor $(b_1\mu_{1_o 3_o})^2$ as well as g_o, as shown in (4), where $(b_1\mu_{1_o 3_o})^2$ is proportional to the measured absorption coefficient. The measured absorption coefficient of the new $N^{15}H_2D$ system was found to be about 0.015 cm^{-1} $Torr^{-1}$, and equal to that for the $N^{14}H_2D$ system. Therefore, for equal microwave power and absorption, the relative gain of the $N^{15}H_2D$ system with respect to the original $N^{14}H_2D$ system is the ratio of the g_o factors alone or

$$\frac{g(N^{15}H_2D)}{g(N^{14}H_2D)} = 1.8 \ .$$

The conversion efficiency ratio varies as the square of the gain ratio for short interaction distances,

$$\frac{\eta(N^{15}H_2D)}{\eta(N^{14}H_2D)} = 3.2 \ .$$

The efficiency of the new system will be 3.2 times that of the original system.

The second new system ($C^{13}O_2^{16}$ R(18), $N^{14}H_3$) promises to have even higher relative parametric gain. Although g_o is only 0.120 (Fig. 6), as compared to the 0.294 for $N^{15}H_2D$, the enhanced absorption of 0.22 cm^{-1} $Torr^{-1}$ for the $N^{14}H_3$ dominates the 0.015 cm^{-1} $Torr^{-1}$ absorption of $N^{15}H_2D$ and $N^{14}H_2D$. The relative parametric gain of the $N^{14}H_3$ system with respect to the other two systems, accounting for the ratios of the measured absorption coefficient as well as the g_o factors, is calculated here. With respect to the $N^{15}H_2D$ system, the gain ratio is

$$\frac{g(N^{14}H_3)}{g(N^{15}H_2D)} = 6.0 \ ,$$

while the relative conversion efficiency is

$$\frac{\eta(N^{14}H_3)}{\eta(N^{15}H_2D)} = 36 \quad ;$$

with respect to the original $N^{14}H_2D$ system, the gain and efficiency ratios are

$$\frac{g(N^{14}H_3)}{g(N^{14}H_2D)} = 11$$

and

$$\frac{\eta(N^{14}H_3)}{\eta(N^{14}H_2D)} = 121,$$

respectively.

The calculation of increased gain for a given microwave input power and absorption, and for a given gas pressure, appears to be valid. A cautionary note concerning the conversion efficiency η is necessary, however. For small parametric interaction distances, the above calculations of conversion efficiency (ratios) are valid. But when appreciable phase mismatch Δk and optical absorption α_3 of the laser beam occur for long interaction distances, further analysis is necessary. The analysis of the coupled parametric equations with high phase mismatch and optical absorption is now in progress.

4. Microwave Stark Cells for the New System

The 4 GHz microwave Stark cell used for the original $N^{14}H_2D$ system will be used for the ($C^{12}O_2^{16}$ P(26), $N^{15}H_2D$) system. Dielectric loading experiments to lower the cavity resonance to the required 2.15 GHz have been initiated.

A 26.378 GHz test cavity has been constructed in order to assess the microwave property of the septum-teflon loaded TE_{107} cavity (Fig. 8). The effects of the entrance and exit holes for the laser beam on the microwave fields need further evaluation; the holes were selected at nodal points of wall current flow. Microwave power will be inserted into the cavity by "hole coupling" the magnetic fields with matching apertures. The laser beam will traverse the cavity at $\sim 30^{\circ}$ to the cavity axis in order that the phase matching of the microwave, laser and parametric output is attained; the angle is set by the cutoff frequency of the cavity. Experiments with multiple reflections of the laser beam on the walls of a 10 cm cavity, in order to increase interaction distances and conversion efficiencies, will be attempted after the preliminary measurements are completed.

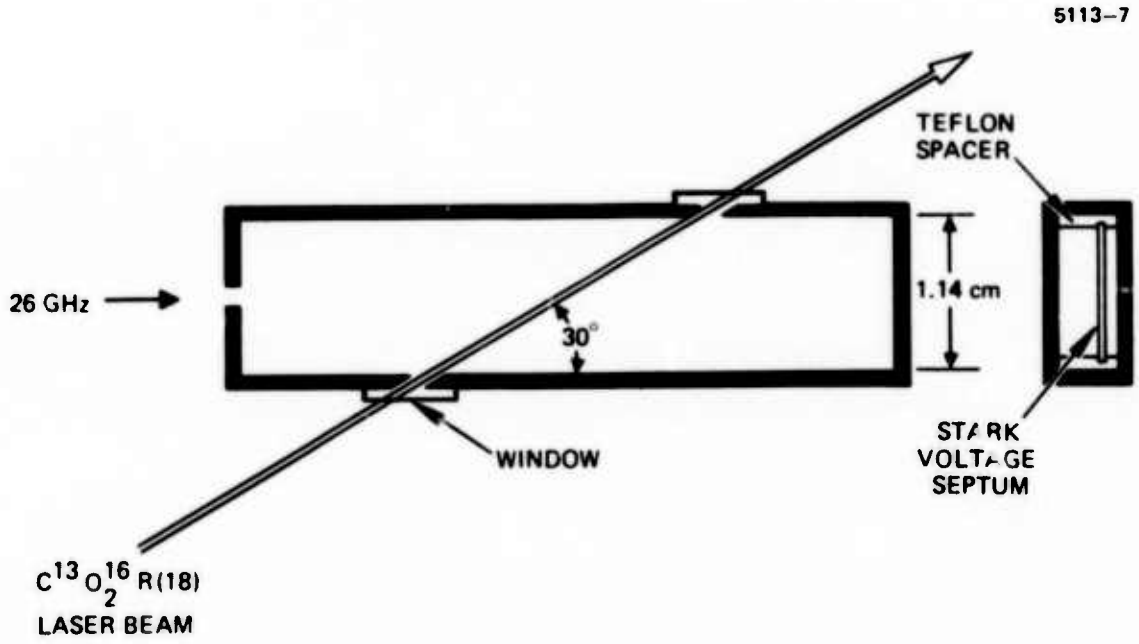

Fig. 8. TE_{107} 26.378 GHz test cavity. The laser beam is passed at 30° in order to phase match the two optical waves to the microwave. The final cavity will be nearly 10 cm long, with multiple passes through the cavity.

APPENDIX A
(To be published)

Stark Induced Two-Photon Mixing in Molecular Gases[+]

R. L. Abrams
Hughes Research Laboratories, Malibu, CA 90265

A. Yariv and P. Yeh[++]
California Institute of Technology, Pasadena, CA 91109

ABSTRACT

Application of a dc electric field to a gaseous system destroys the basic inversion symmetry and allows two-photon mixing processes to occur. A theoretical derivation of this effect under conditions of resonantly enhanced nonlinearities is given for a three-level system. Calculations are presented for mixing of a CO_2 laser with 4 GHz microwaves in the molecule NH_2D, producing single lower sideband radiation.

[+] Supported in part by the Advanced Research Projects Agency, monitored by the Office of Naval Research

[++] Supported by the Army Research Office, Durham, N.C.

Nonlinear optical mixing in atomic vapors has been demonstrated for a number of different processes including third harmonic generation,[1-4] dc induced second harmonic generation,[5,6] infrared upconversion,[7,8] and multiphoton generation of new wavelengths.[9] Resonant enhancement and phase matching of three-photon processes has led to rather impressive conversion efficiencies for certain interactions in atomic vapors.[2-4] In this paper we discuss two-photon mixing processes in molecules where resonant enhancement is achieved via Stark tuning of the molecular energy levels. This interaction and its subsequent experimental observation[10] suggest a new type of electrooptical effect, namely single sideband generation by applied microwave frequencies. Theoretical calculations of the interaction for a three-level system are presented here, specialized to the case of a particular molecule (NH_2D). The experimental observations are discussed in the following paper.[10]

The application of a dc electric field to a gas introduces a preferred spatial direction thus destroying the inversion symmetry. The second order induced polarization amplitude can then be related to the product of the field (complex) amplitudes by

$$P_\alpha^{\omega_1=\omega_3\pm\omega_2} = d_{\alpha\beta\gamma}^{\omega_1=\omega_3\pm\omega_2} E_{3\beta} E_{2\gamma}^{*} \quad . \tag{1}$$

Choosing the direction of the dc field as z, the allowed $d_{\alpha\beta\gamma}$ are d_{zzz}, d_{zii} and d_{izi}, where i = x or y.

In searching for a candidate gas in which to observe the effect one should look for molecules: (1) with a strong permanent dipole moment or (2) molecules which in the presence of a dc field acquire a large dipole moment so that the presence of the dc field constitutes an appreciable perturbation.

A molecule meeting criterion (2) is NH_2D. The molecule has, among others, the three levels shown in Fig. 1, which can be Stark-tuned into simultaneous resonance with the P(20) line of the CO_2 laser[11-14] and microwave radiation near 4.1 GHz as shown. This should lead to a strong resonant mixing of the P(20) line (of frequency $\omega_3/2\pi$) and the microwave field at $\omega_2/2\pi$ = 4.1 GHz, giving rise to the difference frequency radiation at $\omega_1 = \omega_3 - \omega_2$ when the Stark field is near E^{dc} = 3570 V/cm. Levels 1 and 2 belong to the lowest vibrational state ($\nu_2 = 0$) and have molecular angular momentum quantum numbers J = 4 and |M| = 4. The subscripts 04 and 14 correspond to the standard asymmetric top designation.[15] The symbols a (asymmetric) and s (symmetric) refer to the parity of the inversion-split vibrational wave functions. Also shown in the figure are the admixed wavefunctions |1> and |2>. This admixture, which will be shown to be responsible for the nonlinear mixing, disappears at zero dc field. The energy splitting Δ between the two low lying states is

$$\Delta = [4|< 4_{04}a|\mu_z|4_{14}s>|^2(E^{dc})^2 + \delta^2]^{1/2} \qquad (2)$$

where δ is the zero field splitting and μ is the projection of the molecular dipole moment operator along the direction of the dc field.

The expression for the nonlinear dipole moment of an NH_2D molecule depends on matrix elements which can be determined from linear absorption data as well as from the data on Stark splitting. This makes possible, in principle, a precise theoretical derivation of the nonlinear mixing behavior of this molecule and of its parametric dependencies.

Applying second order perturbation theory to the three level system of Fig. 1 and keeping only resonant (i.e., with near vanishing denominator) terms leads to the following expression for the polarization generated at ω_1 by the applied fields at ω_2, ω_3:

$$P_\alpha^{(2)}(t) = \frac{1}{4\hbar^2}\left\{\frac{N_1(\bar{\mu}\cdot\bar{E}_3)_{13}(\bar{\mu}\cdot\bar{E}_2^*)_{21}(\mu_\alpha)_{32}}{[\Gamma_{13}+i(\omega_3-\omega_{31})][\Gamma_{32}+i(\omega_1-\omega_{32})]}\right.$$

$$\left. - \frac{(N_2-N_1)(\bar{\mu}\cdot\bar{E}_3)_{13}(\bar{\mu}\cdot\bar{E}_2^*)_{21}(\mu_\alpha)_{32}}{[\Gamma_{12}+i(\omega_2-\omega_{21})][\Gamma_{32}+i(\omega_1-\omega_{32})]}\right\} e^{i\omega_1 t} \qquad (3)$$

$$+ \text{c.c.}$$

where N_i is the population density of level i with $E_2 = E_3 = 0$. At thermal equilibrium $N_2 \simeq N_1$ and the main contribution to $P_\alpha^{(2)}$ is from the first term, the one proportional to N_1.

At zero dc field the matrix element $(\mu_\alpha)_{32}$ is zero. This is due to the fact that, as can be shown by group theoretic arguments, only the molecular dipole moment along the b of NH_2D axis (μ_b), may possess a non-vanishing matrix element $\langle 5_{05}a|\mu_b|4_{14}s\rangle$, but $\mu_b = 0$ due to the basal plane symmetry of NH_2D. It follows from (3) that for $E^{dc} = 0$ no frequency mixing takes place. When $E^{dc} \neq 0$ the ground state wave function $|4_{04}a\rangle$ is admixed into level 2 as shown in Fig. 1. This results in a non-vanishing matrix element $(\mu_a)_{32}$ proportional to $\langle 5_{05}a|\mu_a|4_{04}a\rangle$.

For $\bar{E}_2 \| \hat{z}$, $\alpha = x$, and $\bar{E}_3 \| \hat{x}$ we can show that the triple matrix element product appearing in (3) is given by

$$(\mu_z)_{21}(\mu_x)_{13}(\mu_x)_{32} = -4\mu_c^2\langle 4_{04}a|\mu_x|5_{05}a\rangle^2 E_{dc} M^2\left(\frac{\delta}{\Delta^2}\right) \qquad (4)$$

The nonlinear mixing is thus absent, i.e., $P_x^{(2)} = 0$, at zero field ($E^{dc} = 0$) and at very high fields ($\Delta \gg \delta$).

From (1) and (3) and using the fact that at room temperature $N_2 \cong N_1$, we obtain

$$d_{\alpha\beta\gamma}^{\omega_1=\omega_3-\omega_2} = \frac{1}{2\hbar^2} \quad \frac{N_1(\mu_\gamma)_{21}(\mu_\beta)_{13}(\mu_\alpha)_{32}}{[\Gamma_{13}+i(\omega_3-\omega_{31})][\Gamma_{32}+i(\omega_1-\omega_{32})]} \tag{5}$$

Expression (5) applies to stationary molecules with energy levels at E_1, E_2 and E_3. In a gas sample we need to account for the Doppler shift of the transition energies of individual molecules. This is done by averaging the nonlinear coefficient $d_{\alpha\beta\gamma}$ over the Maxwellian velocity distribution function with the result for operation at line center, that

$$d_{\alpha\beta\gamma}^{\omega_1=\omega_3-\omega_2} = \frac{-N_1(\mu_\gamma)_{21}(\mu_\beta)_{13}(\mu_\alpha)_{32}}{2\hbar^2} \sqrt{\pi/2} \quad \frac{c}{\sigma\omega_{31}} \quad \frac{\partial F}{\partial \Gamma} , \tag{6}$$

where $F(x) = e^{x^2}\ \mathrm{erfc}(x)$, $\omega_{31} \simeq \omega_{32} >> \omega_{21}$, $\sigma = \sqrt{kT/M}$ is the rms molecular velocity and $x = c\Gamma/(\sqrt{2}\sigma\omega_{31})$, the ratio of the homogeneous (spontaneous plus pressure) linewidth to the Doppler linewidth.

Although a numerical estimate of the nonlinear mixing coefficient based on (6) is possible, a safer procedure and one that serves as a check on the matrix elements needed to evaluate d_{xxz} (the largest coefficient in NH_2D) is to relate it to the linear absorption coefficient for x polarized field at $\omega_3 = \omega_{31}$. The latter can be shown to be given by

$$\gamma_{31} = \gamma_H \sqrt{\pi}\ x e^{x^2}\ \mathrm{erfc}(x) \tag{7}$$

where γ_H is the value of γ_{31} at high pressures ($c\Gamma >> \sigma\omega_{31}$).

Combining (6) and (7) leads after some mathematical manipulation to

$$d_{xxz}^{\omega_1=\omega_3-\omega_2} = -\frac{c(\mu_z)_{12}}{8\pi\hbar\omega_{31}}\left(\frac{\mu_{23}}{\mu_{13}}\right)\sqrt{\frac{\pi}{2}}\ \frac{c\gamma_H}{\sigma\omega_{31}}\left[2x^2F(x) - \frac{2}{\sqrt{\pi}}\,x\right] \qquad (8)$$

The various constants in (8) are evaluated as follows: The matrix element $(\mu_z)_{12}$ is a function of this admixture and is obtained from the wavefunctions of Fig. 1 as

$$(\mu_z)_{12} = \frac{\delta}{\Delta}\,\langle 4_{04}a|\mu_z|4_{14}s\rangle \qquad (9)$$

where the splitting $\Delta = E_2 - E_1$ is given by

$$\Delta = \left[4|\langle 4_{04}a|\mu_z|4_{14}s\rangle|^2(E^{dc})^2 + \delta^2\right]^{1/2} \qquad (10)$$

We obtain the matrix element $\langle a|\mu_z|s\rangle$ from comparing (10) to the experimental tuning curve of ω_{31} vs. $E^{dc(14)}$. This yields $\langle a|\mu_z|s\rangle = 1.14 \times 10^{-18}$ esu. At resonance $E^{dc} = 3570$ V/cm and $\delta/\Delta = 0.174$. The final result is

$$(\mu_z)_{12} = 0.174\langle a|\mu|s\rangle = 0.198 \times 10^{-18} \text{ esu}$$

The saturated absorption γ_H and pressure broadening coefficient are obtained from the data on Ref. (13) as

$$\gamma_H = .028 \text{ cm}^{-1}$$

$$\Gamma/P = 2\pi(20.1 \text{ MHz/Torr}).$$

With these data we obtain

$$d_{xxz}^{\omega_1=\omega_3-\omega_2} = 2.31 \times 10^{-7} G(x) \text{ esu} \tag{11}$$

$$G(x) = 2x\left[\frac{1}{\sqrt{\pi}} - x\, e^{x^2}\, \text{erfc}(x)\right]$$

The theoretical dependence of d_{xxz} on pressure (Eq. 11) is plotted in Fig. 2. The peak occurs at P = 2.0 Torr and has a value of

$$\left(d_{xxz}^{\omega_1=\omega_3-\omega_2}\right)_{max} = 6.4 \times 10^{-8} \text{ esu} = 2.4 \times 10^{-22} \text{ MKS}$$

A comparison of this predicted behavior with experiment is given in the adjoining paper.

The coefficient d estimated above refers to the generation of sideband radiation at ω_1 by mixing a CO_2 P(20) line with a microwave field ω_2 (at 4.1 GHz). It is thus appropriate to compare it to the electro-optic coefficient r_{14} of GaAs which can be used, alternatively, to generate the sideband by conventional electrooptic modulation.

Using the correspondence[16]

$$r_{jlk} = -\frac{2\varepsilon_o}{\varepsilon_j \varepsilon_l} d_{jkl} \tag{12}$$

we have

$$\frac{(n^3 r)_{NH_2D}}{(n^3 r)_{GaAs}} \sim 0.8 \tag{13}$$

We reach the conclusion that for sideband generation, dc biased NH_2D at $P \approx 2$ Torr is comparable to GaAs (which is one of the best infrared modulation materials). We must recognize, however, that this large coefficient was obtained by exploiting the resonant nature of the effect. The penalty we pay for this is that of reduced bandwidth.

The experiment described in the adjoining paper involves traveling wave mixing between an input CO_2 laser (ω_3) and a microwave field at ω_2 ($\sim$4.1 GHz) to generate the difference frequency at $\omega_1 = \omega_3 - \omega_2$. If we neglect saturation, absorption, and take the intensity of the microwave signal to be constant throughout the Stark cell, we can describe the interaction between the fields at ω_3 and ω_1 by[16]

$$\frac{dA_1}{dy} = i \frac{g}{2} A_3 e^{-i\Delta k y}$$

$$\frac{dA_3}{dy} = i \frac{g}{2} A_1 e^{i\Delta k y} \qquad (14)$$

where

$$A_i(y) = \sqrt{\frac{n_i}{\omega_i}} E_i(y)$$

$$g = \sqrt{\frac{\mu_o}{\epsilon_o} \frac{\omega_1 \omega_3}{n_1 n_3}} \, d_{xxz}^{\omega_1 = \omega_3 - \omega_2} E_2$$

$$\Delta k = k_3 - (k_1 + k_2) \qquad (15)$$

Assuming a single input $A_3(0)$ at $x = 0$ and phase-matched operation ($\Delta k = 0$), the solution of (14) is

$$A_1(y) = -iA_3(0)\sin(\frac{gy}{2})$$

$$A_3(y) = A_3(0)\cos(\frac{gy}{2}) \qquad (16)$$

so that a complete transfer of the input power at ω_3 to an output at ω_1 is effected in a distance π/g.

To estimate g we assume $E_2 \sim 4 \times 10^4$ V/m, the field value at which saturation effects are expected. Eq. (15) then gives $g = .007\ cm^{-1}$, resulting complete conversion from ω_3 to ω_1 in an interaction length of $\sim$4.5 m (neglecting absorption). Inclusion of the effects of absorption limit the conversion efficiency to $\sim$5% in this case.

In conclusion, we have shown in detail how Stark admixing can give rise to second order optical nonlinearities in gases. We have derived an expression for the coefficient describing the mixing of an infrared and a microwave field in NH_2D. Available absorption data was used to obtain a numerical estimate for the mixing and to describe its parametric dependence. An experimental demonstration of this effect is described in the following paper.[10]

REFERENCES

1. J. F. Ward and G. H. C. New, Phys. Rev. 185, 57 (1969).
2. J. F. Young, G. C. Bjorklund, A. H. Kung, R. B. Miles, and S. E. Harris, Phys. Rev. Lett. 27, 1551 (1971).
3. A. H. Kung, J. F. Young, G. C. Bjorklund, and S. E. Harris, Phys. Rev. Lett. 29, 985 (1972).
4. K. M. Leung, J. F. Ward and B. J. Orr, Phys. Rev. 9A, 2440 (1974).
5. R. S. Finn and J. F. Ward, Phys. Rev. Lett. 26, 285 (1971).
6. J. F. Ward and Irving J. Bigio, Phys. Rev. 11A, 60 (1975).
7. S. E. Harris and D. M. Bloom, Appl. Phys. Lett. 24, 229 (1974).
8. D. M. Bloom, J. Yardley, J. F. Young, and S. E. Harris, Appl. Phys. Lett. 24, 427 (1974).
9. P. D. Sorokin, J. J. Wynne, and J. R. Lankard, Appl. Phys. Lett. 22, 342 (1973).
10. R. L. Abrams, C. K. Asawa, T. K. Plant, and A. E. Popa, Phys. Rev. Lett. (following paper).
11. R. G. Brewer, M. J. Kelley, and A. Javan, Phys. Rev. Lett. 23, 559 (1969).
12. M. J. Kelley, R. E. Francke, and M. S. Feld, J. Chem. Phys. 53, 2979 (1970).
13. T. K. Plant and R. L. Abrams (unpublished). Earlier data on the absorption coefficient and pressure broadening rate was published by A. R. Johnston and R. O. S. Melville, Appl. Phys. Lett. 19, 503 (1971), but the more recent measurements are more accurate and substantially different.
14. T. A. Nussmeier and R. L. Abrams, Appl. Phys. Lett. 25, 615 (1974).
15. C. H. Townes and A. L. Schawlow, "Microwave Spectroscopy" McGraw-Hill Book Co., Inc. (New York 1955).

16. See, for example, A. Yariv, "Quantum Electronics", J. Wiley and Sons, Inc. (New York, 1975).

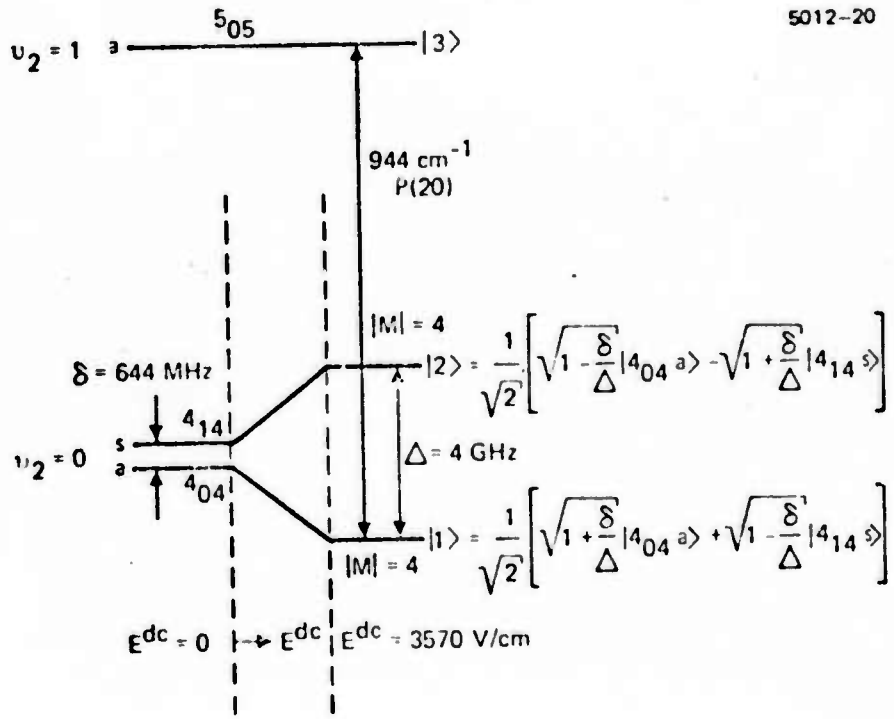

Fig. 1. Some of the energy levels relevant to the derivation of the nonlinear coefficient.

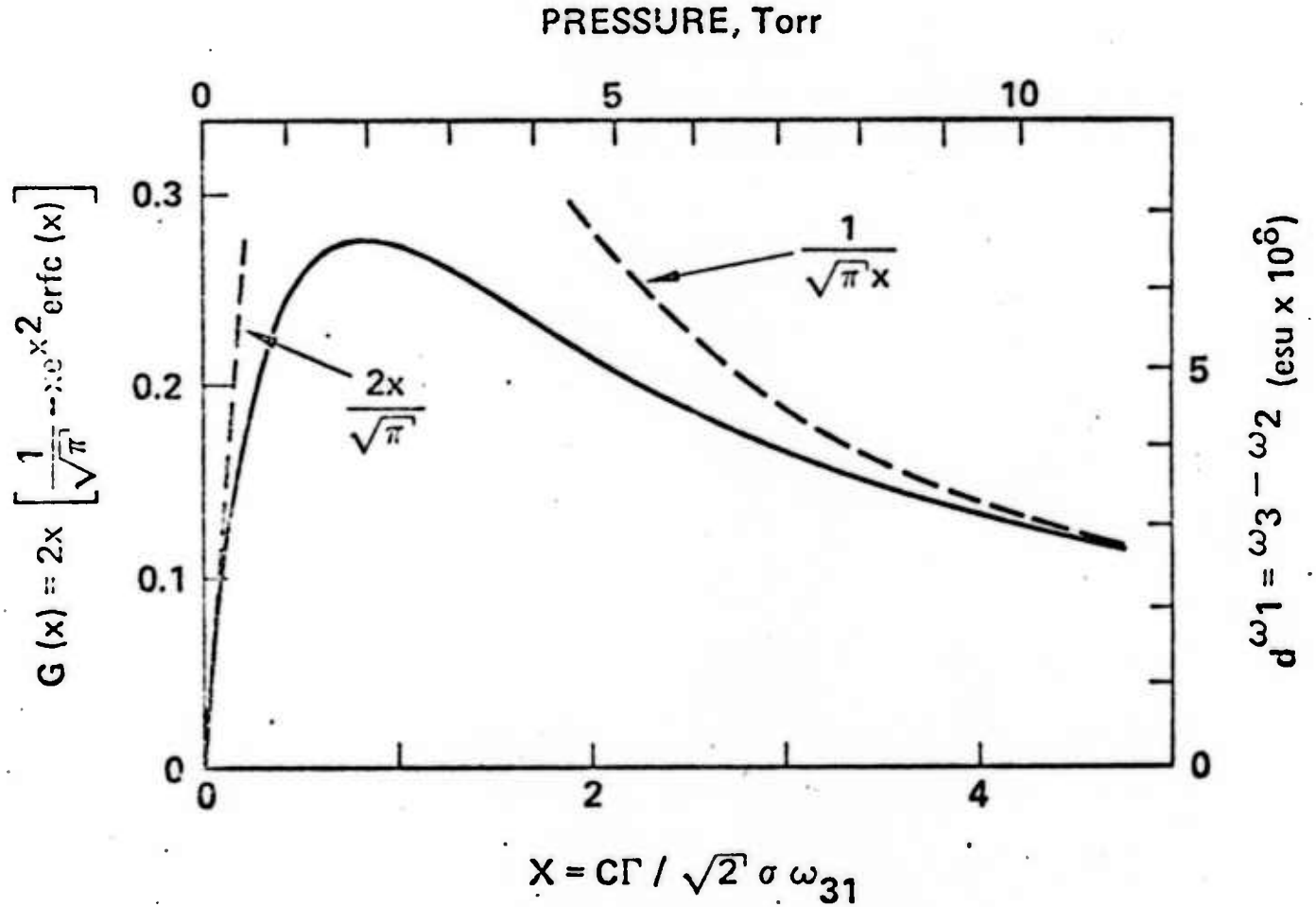

Fig. 2. Theoretical dependence of NH_2D nonlinear coefficient on pressure when the applied fields are exactly resonant with the Stark tuned energy levels.

APPENDIX B
(To be published)

10.6 Micron Parametric Frequency Converter*

R. L. Abrams, C. K. Asawa, T. K. Plant, and A. E. Popa

Hughes Research Laboratories
Malibu, CA 90265

ABSTRACT

The first observation of resonantly enhanced, dc induced, two photon mixing in a gas is presented. A cw CO_2 laser beam and microwave radiation at 4 GHz are mixed in a microwave Stark cell containing gaseous NH_2D. A single new sideband, 4 GHz below the applied CO_2 laser frequency, is observed with the aid of a scanning Fabry-Perot interferometer. The dependence of the sideband signal on gas pressure, microwave frequency, applied dc field, and microwave power are presented and compared with theoretical predictions.

* Research supported in part by the Advanced Research Projects Agency, monitored by the Office of Naval Research.

In the accompanying paper,[1] it was predicted that a resonantly enhanced nonlinear mixing process in the molecule NH_2D could be induced by application of a dc electric field, where CO_2 laser radiation and microwave energy at 4 GHz interact producing a new single sideband 4 GHz below the applied laser frequency. We report here the first experimental observation of such single sideband optical modulation, unambiguously identified through the use of a scanning Fabry-Perot interferometer (SFP). We present measurements of the dependence of the parametric signal on gas pressure, microwave frequency, applied dc field, and microwave power. The results are all in good agreement with theoretical predictions although there is some uncertainty in the quantitative comparisons due to undetermined coupling losses in the microwave structure. Qualitatively, the agreement is excellent.

The experimental apparatus for the observation of the interaction is discussed with reference to Fig. 1. A frequency stabilized cw CO_2 laser beam (operating at P(20) line center) is passed through the microwave Stark cell containing the Stark tunable gas. The cell consists of a 4 GHz ridged waveguide with a 5 mm wide ridge width, a 1.2 mm gap, 20 cm length, and forms a 70 Ω transmission line. The ridge is insulated from the rectangular structure by a thin layer of Teflon, allowing application of a dc Stark voltage and the 4 GHz microwave signal to the ridge. The microwaves are square wave modulated at 2 kHz, amplified in a TWT to 16 W peak power, and coupled into the ridged waveguide by means of a probe. The coupling is adjusted with an external triple stub tuner, where an unknown percentage of the power is lost.

The output of the Stark cell is passed through a SFP and detected with a HgCdTe photodiode. The SFP performs as a narrow bandwidth (300 MHz) optical filter that is slowly scanned through its 10 GHz free spectral range. The SFP output can then either be displayed directly on a recorder or synchronously detected at the microwave modulation frequency in a lock-in amplifier. Very small changes in the SFP output due to the presence of the microwaves were detectable with the latter method.

The NH_2D was prepared by introducing equal partial pressures of NH_3 and ND_3 in a mixing chamber. The resultant mixture containing 37.5% NH_2D was metered into the cell and the pressure monitored with a capacitance manometer.

Figure 2 shows the SFP output before and after lock-in detection with 1.1 Torr of gas in the cell. The two outputs are simultaneously displayed on a strip chart recorder as the SFP is scanned through one full order. The upper trace shows the direct SFP signal, with the familiar pattern of a single mode laser. This is the SFP spectrum of 10.6 μm carrier transmitted through the cell to the detector. The free spectral range (FSR) is 10 GHz (1.5 cm plate spacing). The lower trace of Fig. 2 shows the lock-in detection output with a 30 msec time constant. Signals occur at the positions corresponding to the peaks of the direct SFP output, indicating some sort of carrier modulation as a result of the applied microwave signal. A new peak, which is the parametric signal displaced 4 GHz from the carrier, appears approximately 40% of the way between the two carrier peaks. Note that only a single sideband occurs, for double

sideband generation would result in two signal peaks lying between the two carrier signals. Calibration of the SFP has verified that the sideband is a lower one, as predicted, and corresponds to the difference frequency between the 10.6 μm carrier frequency and the microwave frequency. That the output is a parametric signal and not laser induced fluorescence from the gas is substantiated by the fact that the sideband is linearly polarized and no other line is observed in the SFP output; if the output were fluorescence, unpolarized emission at several wavelengths would be expected.

The parametric signal was measured as a function of the Stark voltage for various microwave frequencies. The SFP sawtooth drive was disconnected and the mirror spacing was set to transmit the peak of the parametric sideband signal for these measurements. The maximum signal occurred at a Stark voltage of 428 V with the microwave frequency set at 4.023 GHz. The full width at half maximum (FWHM) of the signal was 28.5 V which is equivalent to a linewidth of ∿130 MHz. The linewidth of the signal is greater than the NH_2D linewidth at 1 torr of 105 MHz due to some inhomogeneities in the Stark gap.[2] A measured low pressure absorption linewidth of 100 MHz FWHM compared to the 82 MHz actual doppler width indicates a 0.5% variation in the Stark gap spacing.

The Stark voltage was increased to 600 V and the $|M| = 3$ parametric signal was seen at ∿570 V. The ratio of the $|M| = 3$ to the $|M| = 4$ signal amplitudes was 0.414. A theoretical calculation of this intensity ratio yields a predicted signal ratio of .40. The agreement is well within experimental error.

The parametric signal was measured as a function of the Stark cell pressure over a range of 0 to 8 torr as shown in Fig. 3. The SFP was set to transmit the maximum signal and the microwave frequency was fixed at 4.023 GHz. The parametric signal rose slowly between 0 and 0.5 torr, then rose sharply between 0.5 and 1.5 torr, reaching a maximum at 2.4 torr. The signal slowly decreased between 3 and 8 torr. The experimental curve and theory[1] were compared using the best current NH_2D parameters with the theoretical points also shown on Fig. 3. Here the experimental "effective" doppler width of 100 MHz was used to include the effects of the gap inhomogeneities. Again, the excellent agreement enforces the theory.

Figure 4 shows the experimental dependence of parametric signal versus microwave power. For these measurements, the microwave frequency was 4.023 GHz and the Stark voltage was set for maximum signal. The conversion efficiency η is given by the expression

$$\eta = \sin^2\left(\frac{gx}{2}\right)$$

$$\simeq \frac{g^2x^2}{4}$$

where g is the parametric gain and x is the interaction length. The approximation is valid for small values of gx. In the absence of microwave power saturation, g is proportional to the microwave field and η should vary linearly with the microwave power. At high power levels, when the microwave perturbation is comparable to the absorption linewidth ($\mu \cdot E_{RF} \sim 100$ MHz), we expect to observe saturation of the conversion efficiency. Clearly, the applied fields in this experiment are much less than this value.

A crude estimate of the microwave electric field causing the nonlinear mixing may be made under some simplifying assumptions. With 16 W of applied power, noticeable heating of the triple stub tuner and input connector was observed indicating that a significant amount of power was lost. If we assume a 50% power loss, the peak RF electric field across the 0.12 cm gap was 19.7 kV/m. This would result in a conversion efficiency of 0.12% in the 20 cm interaction length. The observed conversion efficiency was 0.1%, in excellent (if not foruitous) agreement considering the uncertainty in the applied microwave field. The experiment is now being redesigned with a resonant microwave cavity (made up of a shorted ridged waveguide). Careful Q measurements and improved matching techniques will result in higher conversion efficiency with lower microwave power and a more accurate experimental determination of the nonlinear coefficient.

In conclusion we have observed a new type of electrooptic effect, namely single sideband infrared generation due to resonantly enhanced, dc induced, two photon mixing in a gas. In the future we hope to increase the conversion efficiency to useful levels, although cw power levels suitable for local oscillator applications could be generated with the present device.

The authors wish to acknowledge the able technical assistance of R. E. Brower and R. R. Niedziejko in carrying out these experiments.

REFERENCES

1. R. L. Abrams, A. Yariv, and P. Yeh, Phys. Rev. Lett. (preceding paper).

2. T. K. Plant and R. L. Abrams (unpublished).

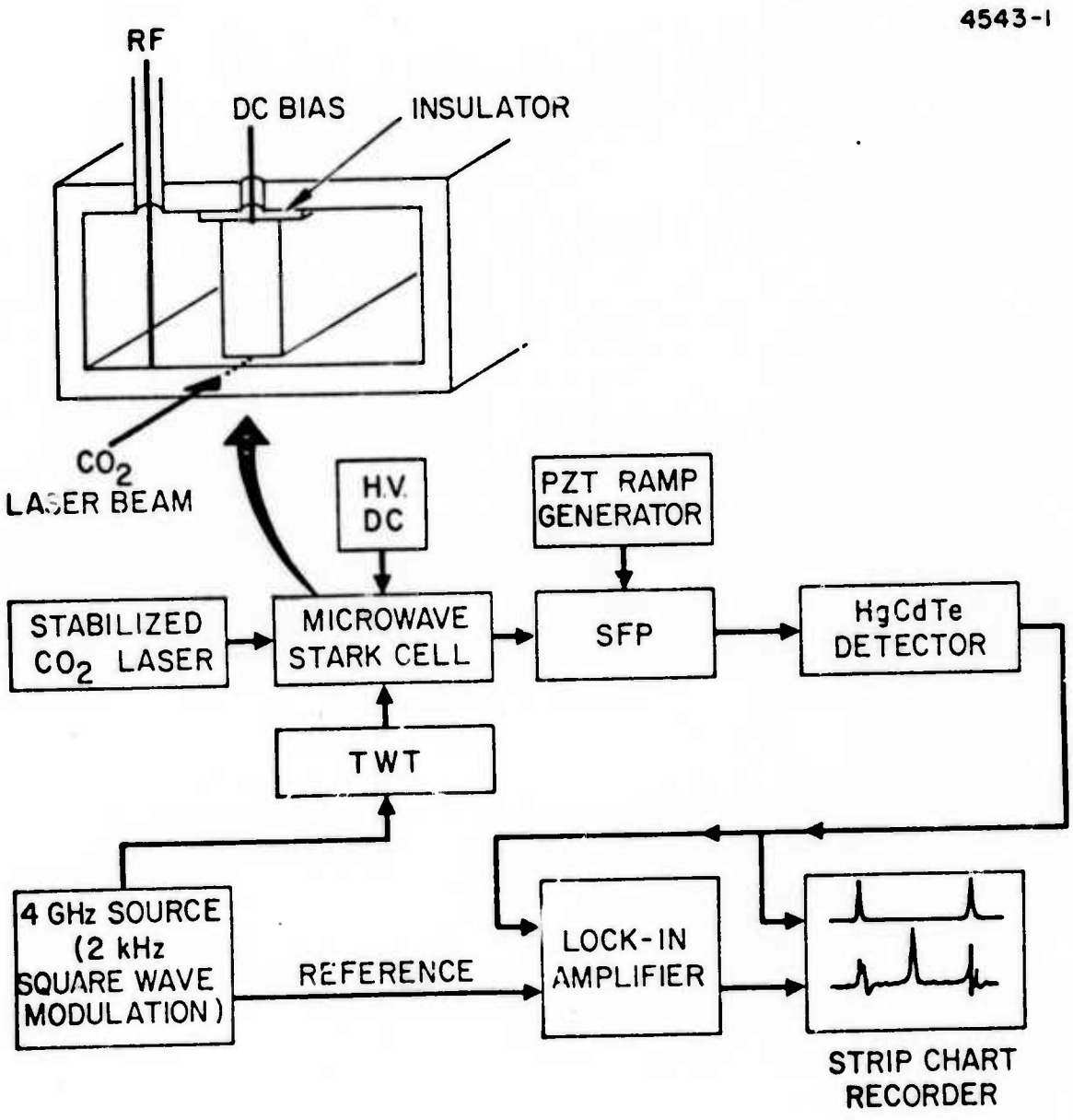

Fig. 1. Experimental apparatus for observation of single sideband signal. The traveling wave tube amplifier (TWT) supplies up to 16 W to the Stark cell.

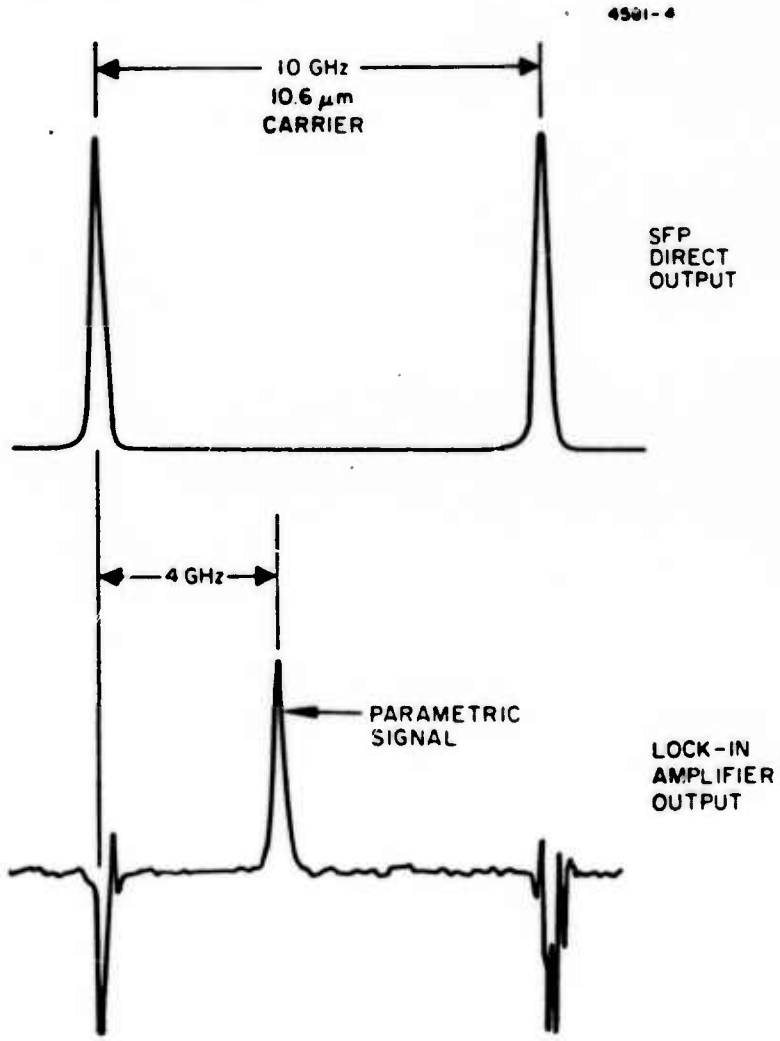

Fig. 2. Simultaneous signals observed
(a) Directly from the detector.
(b) After phase sensitive detection as the SFP is scanned through one order. Note that the new feature due to the 4 GHz microwave signal appears as a single sideband 4 GHz away from the carrier.

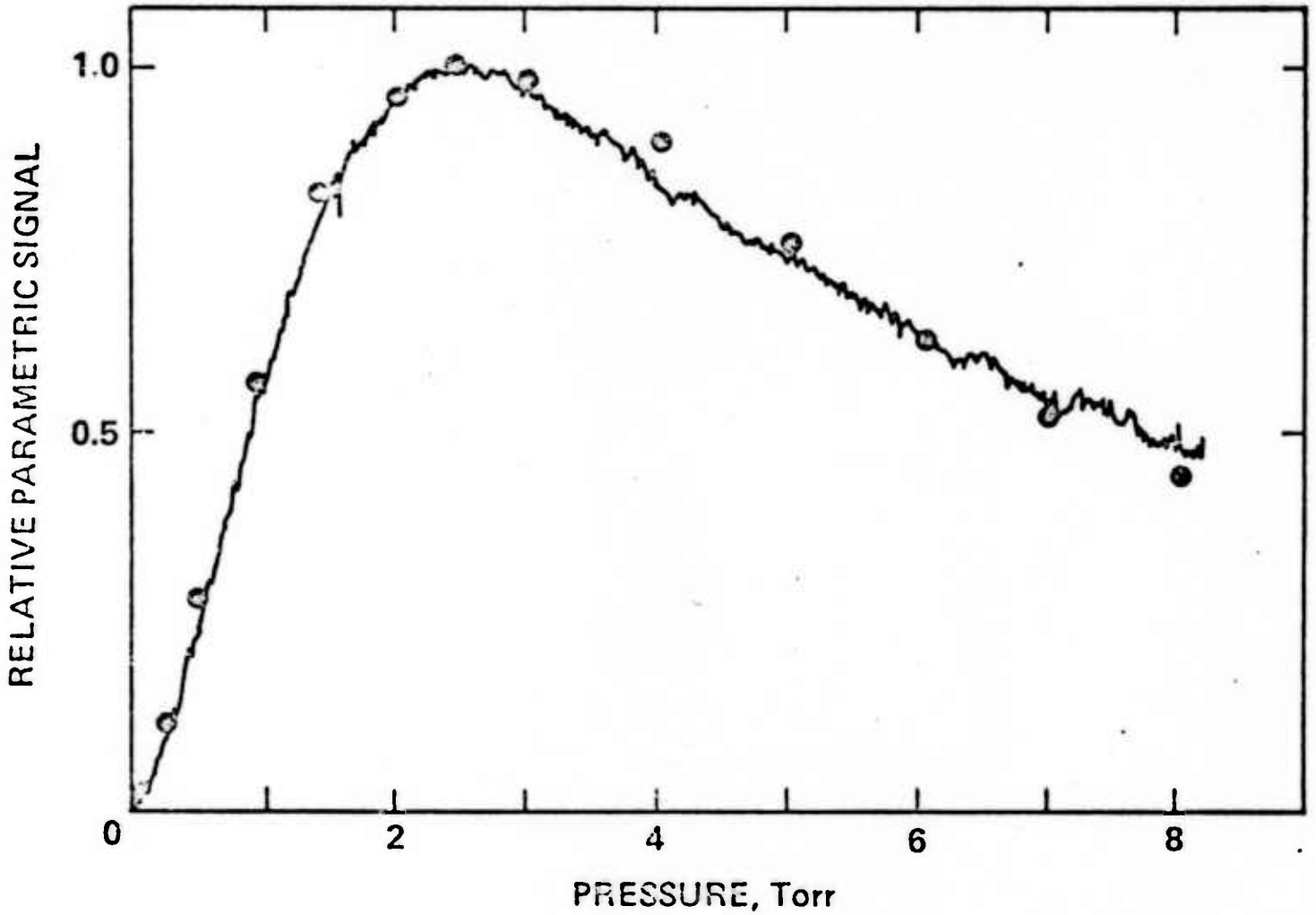

Fig. 3. Parametric signal versus Stark cell pressure 0 to 8 Torr. The theoretical points are calculated for a pressure broadening coefficient of 40.2 MHz/Torr with an effective Doppler width of 100 MHz.

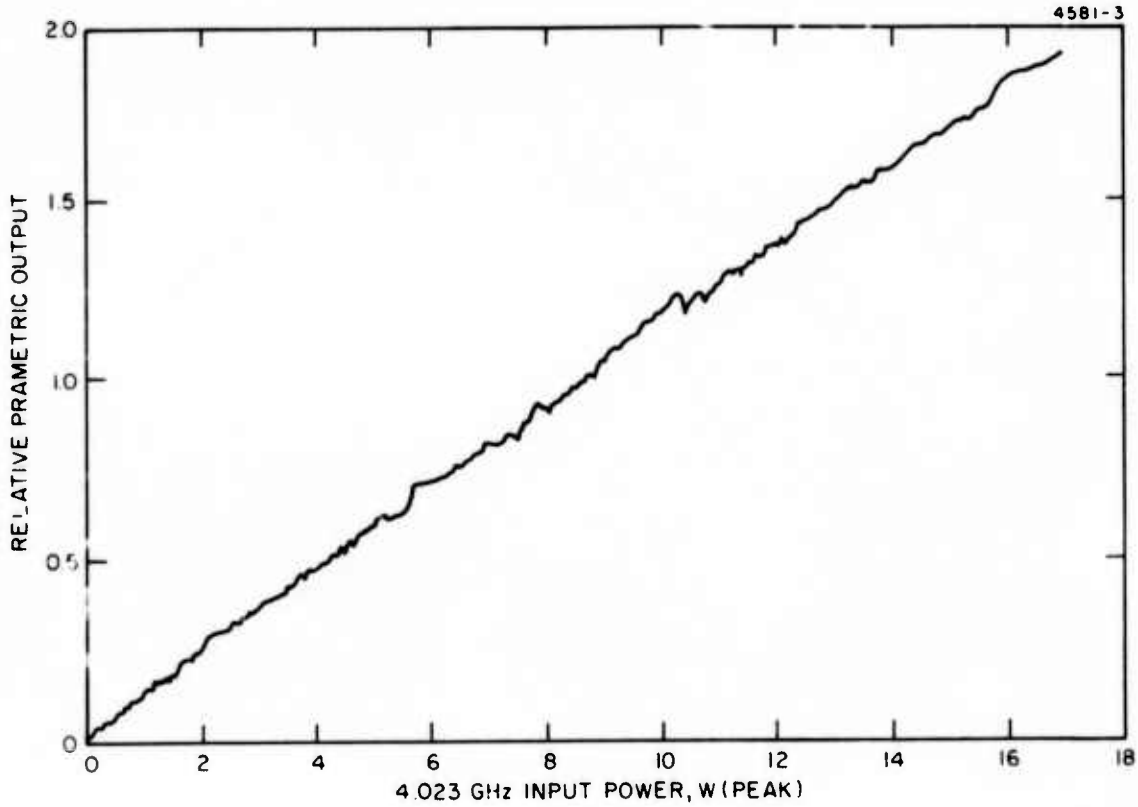

Fig. 4. Parametric signal versus microwave power.

APPENDIX C
(To be published)

Broadening and Absorption Coefficients in $N^{14}H_2D$

T. K. Plant and R. L. Abrams

Hughes Research Laboratories
Malibu, California 90265

ABSTRACT

The magnitudes of the pressure broadening and linear absorption coefficients have been measured for the Stark tunable $(0_a, 4_{04}, 4) \rightarrow (1_a, 5_{05}\, 5)$ transition in $N^{14}H_2D$ using a CO_2 laser operating on the P(20) 10.59 μm line. Two separate analysis methods give consistent results which are substantially different from values previously reported.

Broadening and Absorption Coefficients in $N^{14}H_2D$

T. K. Plant and R. L. Abrams

Hughes Research Laboratories
Malibu, California 90265

The interaction of CO_2 laser radiation with Stark tunable absorption lines in molecules is proving to be of importance for CO_2 laser communications systems. Due to its unique energy level structure $N^{14}H_2D$ has proven useful for laser modulation,[1] laser stabilization,[2] and, more recently, nonlinear optical interactions whereby a single sideband modulator operating at microwave frequencies was demonstrated.[3] For each of these applications it is necessary to know accurately both the magnitude and the linewidth of the absorption coefficient as a function of pressure. Johnston and Melville[1] reported values of .042 cm^{-1} for the high pressure line center absorption coefficient and 64 MHz/Torr full width half maximum (FWHM) for the pressure broadening coefficient. However, their Stark plate spacing showed a large nonuniformity evidenced by a measured low pressure linewidth of 200 MHz FWHM in comparison with an expected Doppler width of 82 MHz.

In this paper we report new values for these parameters which were obtained by two separate methods. The absorption lineshapes were fit to a Voigt profile from which the homogeneous linewidths were extracted. Secondly, the line center absorption coefficients, corrected for overlapping $|M| = 3$ absorption, were plotted as a log-log function of pressure from which the pressure broadening coefficient was calculated. The agreement in the results from the two methods is excellent.

The experimental arrangement is shown in Fig. 1. The CO_2 waveguide laser source is Stark stabilized[2] at line center of the P(20) 10.6 μm transition. One plate of the St bsorption cell is grounded while the other plate is driven by a 9 Hz 300 V peak to peak square wave imposed on a slow sawtooth sweep varying from 240-350V. Thus as the ramp voltage increases, the peak of the square wave is swept through the $|M| = 4$ absorption of the $(0_a,4_{04},4) \rightarrow (1_a,5_{05},5)$ transition in $N^{14}H_2D$ whose center is at 450V Stark voltage for our cell with a gap of 0.127 cm. The output of the Hg(Cd)Te detector is then phase sensitively detected at the 9 Hz square wave reference frequency. This low frequency is required due to the limited slewing rate of the high voltage operational amplifier which must provide a very sharp voltage rise relative to the pulse width in order to avoid the gradual application of the resonant Stark voltage.

The total, unabsorbed CO_2 signal level is found by chopping the laser beam with no applied Stark voltage and remains very stable during a run. Adequate attenuation is provided to avoid any power broadening in the gas or saturation of the detector. A slow sweep through the $N^{14}H_2D$ Stark resonance is made for gas pressures ranging from 50 μm to 10 Torr yielding recorder plots of the corresponding absorption lineshapes. By holding the laser frequency fixed and varying the Stark voltage to sweep through the absorption, problems of variation in laser intensity or detector sensitivity with frequency are avoided.

Since the $|M| = 3$ absorption in $N^{14}H_2D$ lies only 150V or ~670 MHz above the $|M| = 4$ absorption, corrections must be made for the additional contribution of $|M| = 3$ to the total absorption at higher pressures. This

correction ranges from less than 1% at 4.5 Torr to ~7.5% at 10 Torr and was found from a series expansion of the total absorption given by

$$A_{total} = (1-e^{-\gamma_4 \ell}) + (1-e^{-\gamma_3 \ell})$$

where γ_i is the absorption coefficient due to the $|M| = i$ transition and ℓ is the length of the Stark absorption cell. In this case $\ell = 10$ cm. The absorption coefficients are proportional to the lineshape function times a factor giving the relative intensities of the Stark components.[4]

The $N^{14}H_2D$ is formed by mixing two parts $N^{14}H_3$ and one part $N^{14}D_3$ (98 atomic percent purity) and storing the resultant mix in a stainless steel cylinder for future use. Evidence points to almost immediate mixing of these two species to yield a statistical mix of products of which ~45% is NH_2D. There is also evidence of changes in the gas composition over especially the first few minutes in the Stark cell.

The cell consists of two pieces of precision ground Al_2O_3, gold plated in the center electrode region, which are mated together and sealed in a stainless steel can with small ZnSe AR coated windows. Since NH_3 is known to adsorb to many surfaces, especially heavy metals, it is possible that any or all of the components are adsorbed to some extent thus changing the pressure in the cell. This was evidenced by a rapid decrease of up to 75% in the pressure of a clean cell filled with gas and sealed. If localized heating of the plates occurs from heating by the laser, there could even be breakdown products like N_2 or H_2 gases in the cell.[5] For the data presented here, however, care was taken to attenuate the laser and to allow time at each pressure for equilibration of the gas, so these processes should not affect the results.

In fitting the lineshape data to a Voigt profile to extract the homogeneous linewidths the Doppler width must be specified. The theoretical Doppler width for $N^{14}H_2D$ at room temperature is 82 MHz FWHM. However, a variation in the nominal 50 mil Stark gap spacing of only 0.18 mil is enough to add 5 MHz to the apparent Doppler width. Since our low pressure ($\sim$50 μm) apparent Doppler width was 86 ± 3 MHz, we decided to fit the data to a Voigt profile over a range of inhomogeneous widths from 82-89 MHz and pick those values from the best fit consistent with our measured value.

A computer program was available to fit the data to a Voigt profile.[6] Figure 2 shows the generated best homogeneous linewidths for various pressures and the best straight line fit through zero to these values. The rms error in the fits is less than 3% while the resulting linewidth error is less than 2%. The error bars are points at which the rms fitting error becomes twice its minimum value. The effective Doppler width giving the best straight line through zero is 84.5 MHz which agrees with our measured value within experimental error. The slope of the line is the pressure broadening coefficient of 40.2 ± 0.4 MHz/Torr.

A second determination of the pressure broadening coefficient is made by examining the pressure dependence of the line center absorption coefficient.[7] The line center absorption coefficient in the high pressure Lorentzian region is given by

$$\gamma(\lambda_o) = -\frac{1}{8\pi}\frac{\lambda_o^2}{\tau_{21}}\left(\frac{2}{\pi\Delta\nu_L}\right)\left[N_2 - \frac{g_2}{g_1}N_1\right]$$

where τ_{21} is the radiative lifetime of the transition, λ_o is its wavelength, $\Delta\nu_L$ is the homogeneous linewidth (FWHM) and is proportional to pressure, and N_2 and N_1 are the populations of the upper and lower energy levels respectively. Since N_2 and N_1 are also proportional to pressure, the pressure dependence cancels that of $\Delta\nu_L$ leaving $\gamma(\lambda_o)$ a constant.

In the low pressure Doppler limit the line center absorption coefficient is given by

$$\gamma(\lambda_o) = -\frac{1}{8\pi}\,\frac{\lambda_o^2}{\tau_{21}}\,\frac{2}{\Delta\nu_D}\sqrt{\frac{\ell n\ 2}{\pi}}\left[N_2 - \frac{g_2}{g_1}N_1\right]$$

where $\Delta\nu_D$ is the Doppler broadened linewidth FWHM. Since $\Delta\nu_D$ is constant, $\gamma(\lambda_o)$ varies linearly with pressure as N_2 and N_1. Figure 3 is a log-log plot of $\gamma(\lambda_o)$ versus total cell pressure showing the linear behavior expected in both high and low pressure limits.

The Voigt lineshape leads to the following relation for the line center absorption coefficient

$$\gamma(\lambda_o) = -\frac{1}{8\pi}\,\frac{\lambda_o^2}{\tau_{21}}\,\frac{a}{\Delta\nu_L\sqrt{\pi}}\left[N_2 - \frac{g_2}{g_1}N_1\right]\left[1 - \mathrm{erf}\ a\right]e^{a^2}$$

where $a = \dfrac{\Delta\nu_L}{\Delta\nu_D}(\ell n\ 2)^{1/2}$ and erf is the error function.[8] Using the values of $\Delta\nu_D$ = 84.5 MHz and 40.3 MHz/Torr for the pressure broadening coefficient in the above equation gives the curve shown in Fig. 3, which is an excellent fit to the experimental points.

The effective Doppler width (inhomogeneous linewidth) of 84.5 MHz is a combination of a theoretical 82 MHz Doppler width with ~2.5 MHz of broadening due to inhomogeneities in the Stark field of the absorption cell. Also shown in Fig. 3 is the predicted asymptotic behavior of the

line center absorption coefficient at both high and low pressures. The pressure broadening coefficient is 40.2 ± 0.4 MHz/Torr and the high pressure limit of the $|M| = 4$ transition line center absorption coefficient is found to be 0.028 cm^{-1}. Recent measurements of the transition dipole moment and collision rate using the Carr-Purcell echo technique are in excellent agreement with these values.[9]

In summary, we have used a fixed frequency source and a varying Stark field to trace out the $N^{14}H_2D$ absorption linewidths. From Voigt profile fits to the lineshapes and from the line center absorption coefficients, values of the pressure broadening coefficient and the high pressure absorption coefficient were found to be in good agreement. These more accurate values for this $N^{14}H_2D$ transition should prove valuable in the design of Stark cell devices for applications to problems in optical communications.

The authors are grateful for helpful discussions with C. K. Asawa and G. L. Tangonan and for the excellent technical assistance of R. E. Brower.

REFERENCES

1. A. R. Johnston and R. D. S. Melville, Jr., Appl. Phys. Lett. 19, 503 (1971).
2. T. A. Nussmeier and R. L. Abrams, Appl. Phys. Lett. 25, 615 (1974).
3. R. L. Abrams, C. K. Asawa, T. K. Plant, A. E. Popa, A. Yariv, and P. Yeh, 1976 International Quantum Electronics Conference, paper Q-5, Amsterdam, The Netherlands, June 1976.
4. C. H. Townes and A. L. Schawlow, Microwave Spectroscopy (McGraw-Hill, New York, 1955), p. 256.
5. P. T. Dawson and R. S. Hansen, J. Chem. Phys. 48, 623 (1968).
6. R. L. Abrams, Appl. Phys. Lett. 25, 609 (1974).
7. E. T. Gerry and D. A. Leonard, Appl. Phys. Lett. 8, 227 (1966).
8. T. K. McCubbin and T. R. Mooney, J. Quantum Spectrosc. Radiat. Transfer 8, 1225 (1968).
9. R. L. Shoemaker and E. W. Van Stryland, private communication.

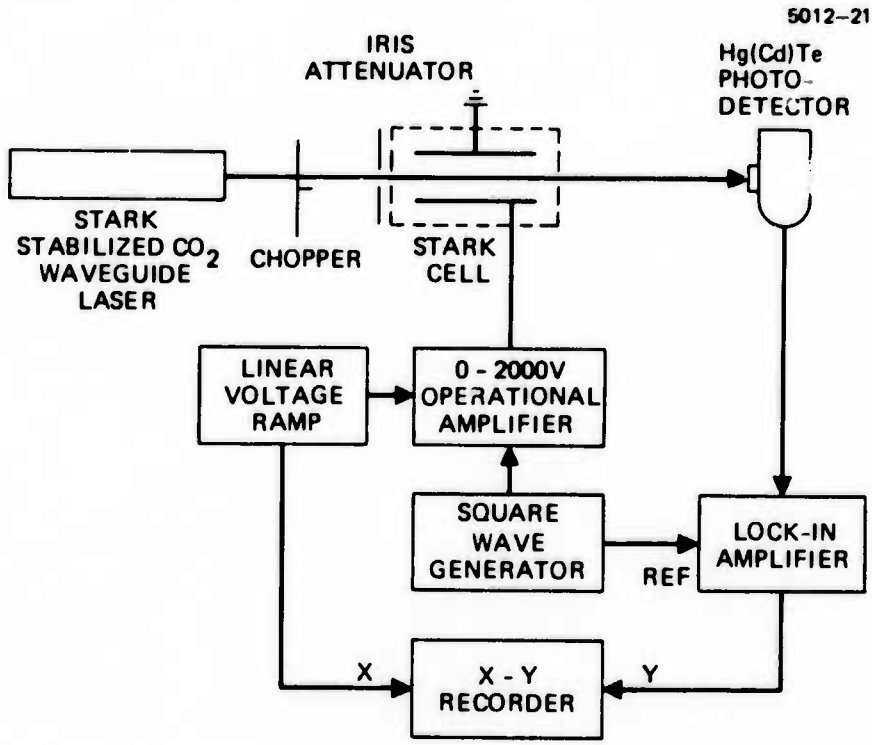

Fig. 1. Experimental arrangement for measuring absorption coefficient and linewidth of $N^{14}H_2D$ absorption.

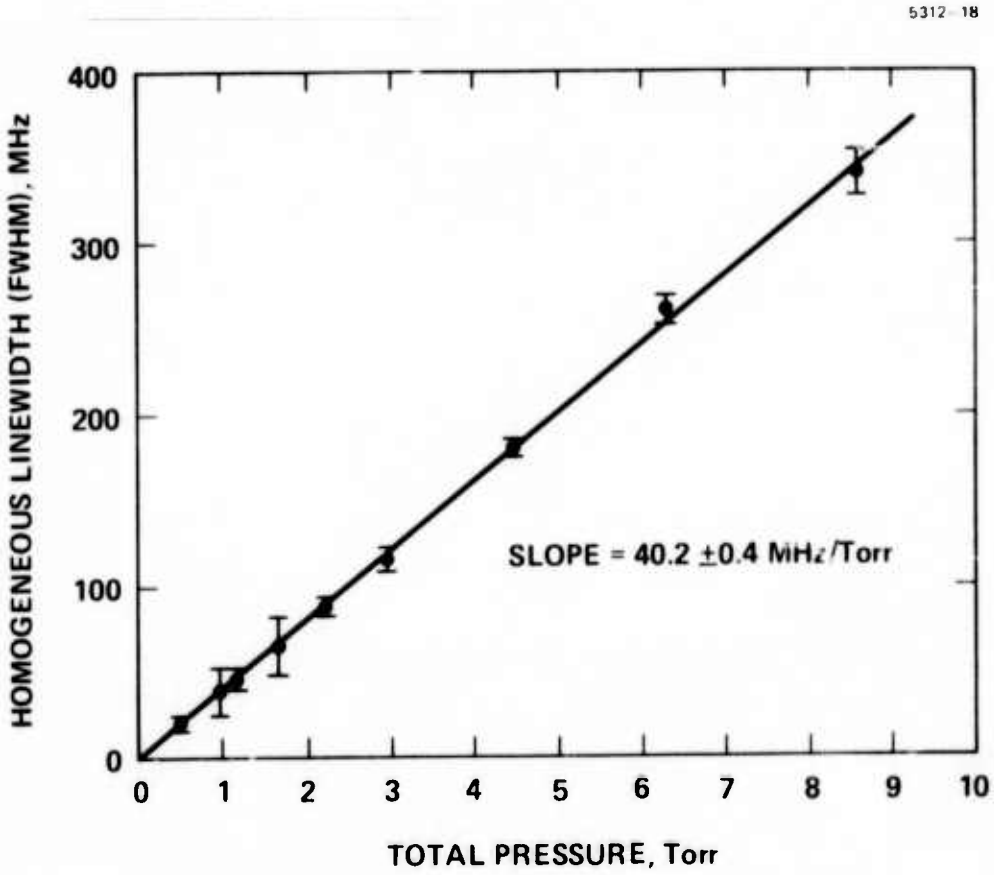

Fig. 2. Homogeneous linewidth extracted from Voigt profile fit to absorption lineshapes versus Stark cell pressure. Effective $\Delta\nu_D$ = 84.5 MHz (FWHM). Slope yields pressure broadening coefficient.

5312-19

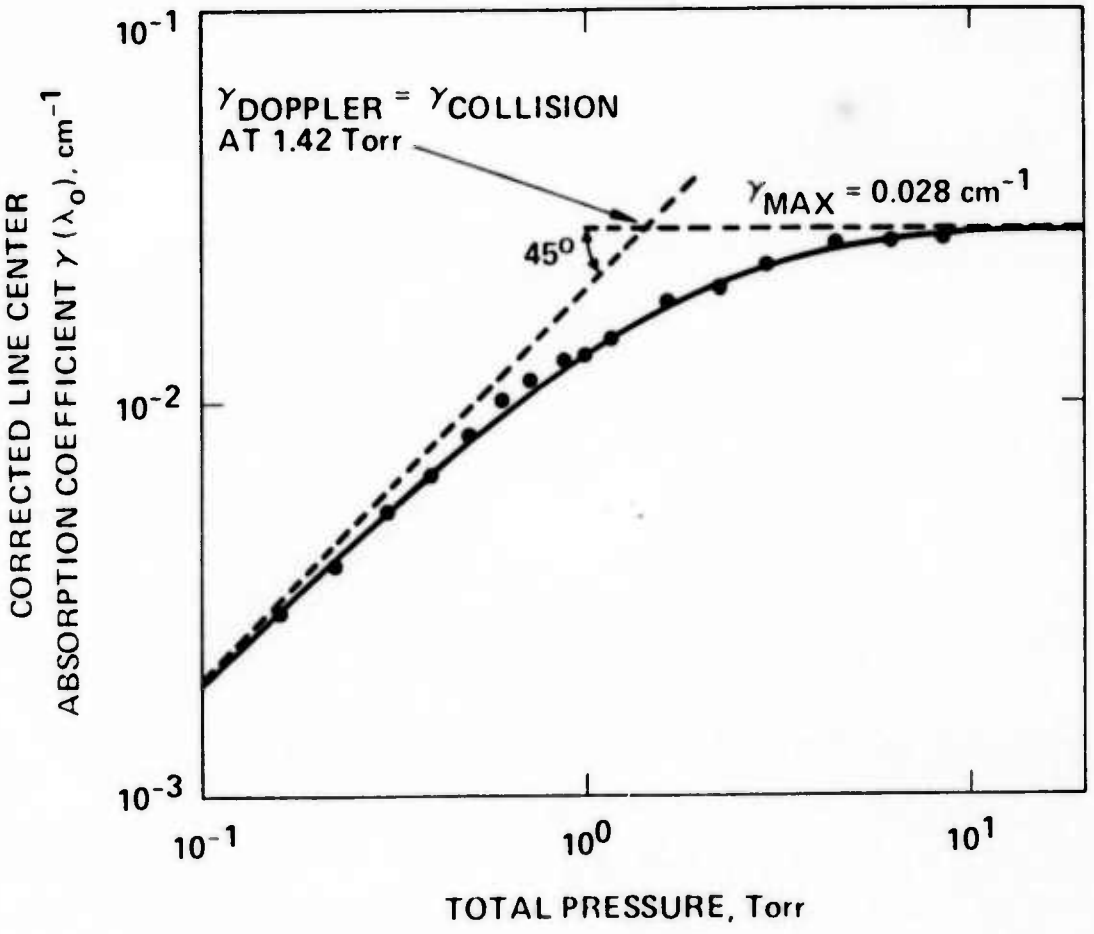

Fig. 3. Corrected line center absorption coefficient ($|M| = 3$ effects subtracted) versus Stark cell pressure. Solid line is dependence predicted from Voigt profile using $\Delta\nu_D = 84.5$ MHz and $\Delta\nu_L = 40.3$ MHz/Torr.

APPENDIX D
(To be published)

STARK TUNED RESONANCES OF $N^{15}H_2D$ WITH CO_2 LASER LINES

G. L. Tangonan and R. L. Abrams

Hughes Research Laboratories
3011 Malibu Canyon Road
Malibu, California 90265

ABSTRACT

The CO_2 laser spectroscopy of mixtures of $N^{15}H_2D$ and $N^{15}HD_2$ gas has been studied. Four new resonances with the P(28), P(26), P(10) and R(18) lines have been observed. The applicability of these new resonances to Stark cell stabilization of CO_2 lasers is discussed.

STARK TUNED RESONANCES OF $N^{15}H_2D$ WITH CO_2 LASER LINES

G. L. Tangonan and R. L. Abrams

Hughes Research Laboratories
3011 Malibu Canyon Road
Malibu, California 90265

Stark tunable resonance absorption of CO_2 laser radiation in $N^{15}H_2D$ has been studied for application to laser stabilization. Resonant electric field strengths and Stark tuning rates (MHz/V/cm) are reported for four new transitions and a summary of transitions in $N^{14}H_2D$ and $N^{15}H_2D$ suitable for CO_2 laser stabilization is presented.

Frequency locking of a GHz tunable waveguide CO_2 laser[1] to a Stark tunable absorption line has recently been demonstrated.[2] This simple technique eliminates the need for frequency modulation of the laser normally used to generate a frequency discriminant and, furthermore, allows one to lock the laser off of line center at any frequency within the laser tuning range. Using $N^{14}H_2D$, a waveguide CO_2 laser operating on the P(20) 10.59 μm transition was stabilized and tuned over its GHz tuning range. Other CO_2 laser transitions in the 00^01 - 10^00 band which can be stabilized using $N^{14}H_2D$ are P(14) and R(12).

In this paper we report the observation of new Stark tunable resonances in mixtures of $N^{14}D_3$ and $N^{15}H_3$ using a CO laser operating in the 00^01 - 10^00 vibrational band. Due to H-D exchange collisions, the gas mixture contains $N^{14}H_2D$, $N^{15}H_2D$, $N^{14}HD_2$, $N^{15}HD_2$ as well as the original constituents. The resonant electric field and its dependence on laser frequency relative to line center have been measured, yielding the Stark tuning rate in MHz/V/cm, which along with the measured J values and calculated dipole moments provides a clue to the identification of the

molecular species involved. A summary of all observed transitions, including the previously measured $N^{14}H_2D$ lines, the Stark tuning rates, and approximate values for the line center absorption coefficient is presented, as well as a discussion of their suitability for CO_2 laser stabilization.

The Stark cell constructed for these experiments is an improved version of the simple glass cells used previously.[2] The Stark plates are evaporated gold on Al_2O_3 ceramic and are enclosed in a stainless steel cell. The leads contacting the Stark plates are completely insulated to prevent gas breakdown. The plate spacing is 0.127 cm and the cell length is 10 cm. The cell is filled with 1:1 mixture of $N^{15}H_3$ and $N^{14}D_3$ to a total pressure of 1 Torr. At this pressure gas breakdown does not occur at voltages below 1000 V.

A conventional CO_2 laser equipped with a diffraction grating as one reflector and a partially transmissive mirror mounted on a piezoelectric crystal as the opposite reflector was used in the initial search for laser coincidences. Laser operation on single lines from P(40) to P(8) and R(8) to R(40) of the $00^0 1 - 10^0 0$ band, was directed through the cell and detected with a (HgCd)Te detector. A slow voltage ramp raised one Stark plate voltage from 0 to 1000 V, while an ac modulation of 10 KHz amplitude 10 V was applied to the opposite plate. The output of the detector was phase sensitively detected with respect to the 10 KHz external reference. The lock-in amplifier output has the usual first derivative line shape and could serve as the frequency discriminant for a laser frequency control servo-loop.

New Stark tuned laser resonances due to the presence of N^{15} have been observed on the P(26), P(10) and R(18) lines for the field strengths used (up to 7.87 kV/cm). The lock-in output for these resonances is shown in Fig. 1. From the voltage ratio of successive resonances, the $|M|$ values

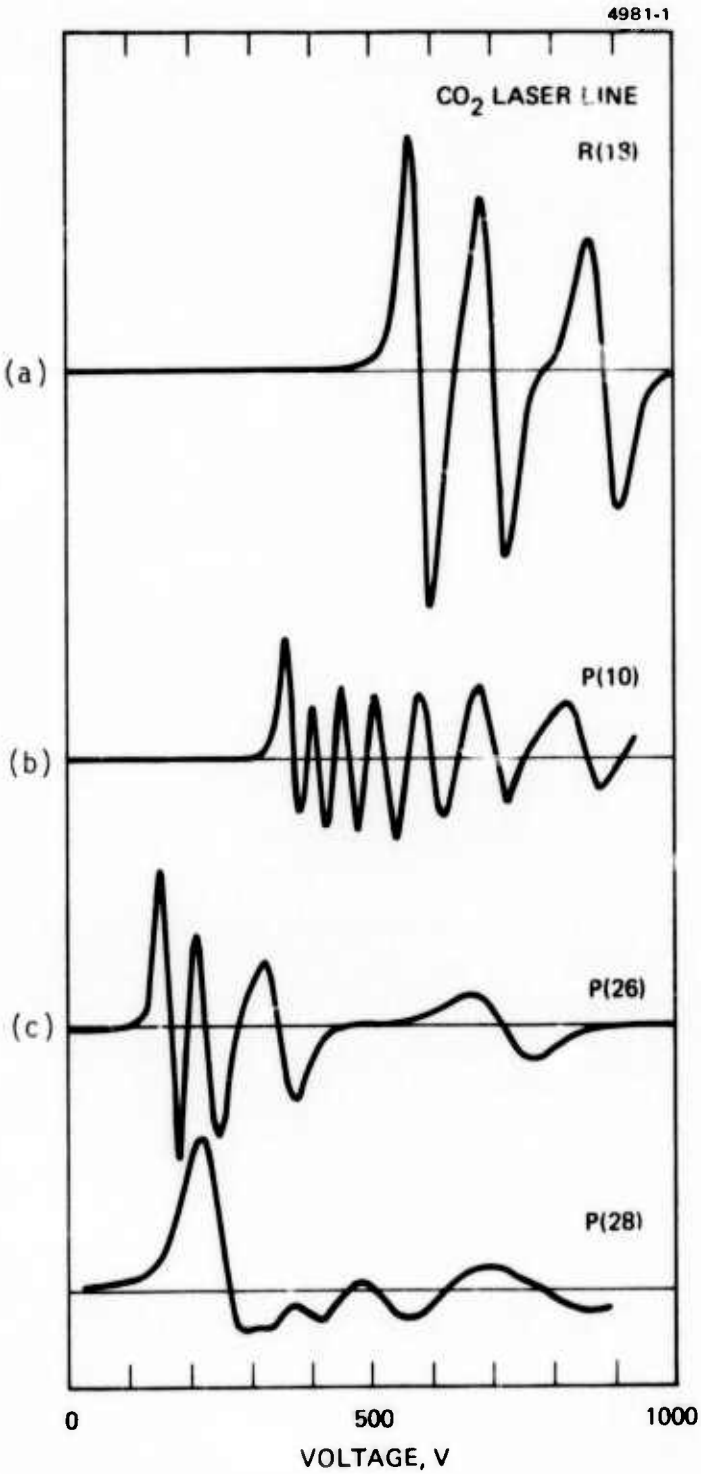

Fig. 1. Stark tuned resonances of a 50:50 $N^{15}H_3 + N^{14}D_3$ gas mixture. The Stark plate spacing was 0.127 cm.

and J values of the states involved in the Stark tuning can be assigned except for the P(28) line, where this is not possible due to the complex resonance trace. For the other resonances this identification is straightforward. The strongest resonances occur on R(18) and P(26) and it is clear from the traces that these can be used in laser frequency control quite readily. For these two resonances, the $N^{15}H_3$:$N^{14}D_3$ ratio was varied keeping 1 Torr total pressure. A maximum in the % absorption occurs for a 2:1 mixture. This indicates that perhaps the $N^{15}H_2D$ species is responsible for these coincidences. No reports of these observed resonances have been given for the molecules $N^{15}H_3$, $N^{14}H_2D$ and $N^{14}HD_2$ which have ν_2 vibrations in this energy range.[4]

The Stark tuning rate for the coincidences has been measured using a heterodyne experiment. Two lasers were used with one laser fixed at line center and the other laser was varied in frequency ±30 MHz about line center. The Stark cell with the gas mixture (1:1) was placed in the arm of the circuit containing the variable frequency laser. The voltage shifts necessary to keep the $|M| = J$ line in resonances as the laser frequency was varied about line center is a measure of the Stark tuning rate. A knowledge of this parameter is crucial to evaluating the usefulness of these resonances for frequency stabilization as well as for spectroscopic identification of the Stark tuning states and upper states of the laser induced transition. The results of the measurements are given in Table 1 with the assigned J values and the position of the $M = J$ resonance for the coincidences observed, in addition the results measured for $N^{14}H_2D$ resonances are included.

Unlike the case for $N^{14}H_2D$ gas, very little work has been done on the microwave and infrared spectra of $N^{15}H_2D$ and $N^{15}HD_2$. Estimates of the zero field splitting between the two interacting levels can be obtained from the measured tuning rates and position of the M = J resonance. In an asymmetric top molecule, the dipole moment between two interacting rotational states J_ν and J_ν, is given by[3]

$$\mu_{12} = \mu \frac{M}{\sqrt{J(J+1)(2J+1)}} S_{J_\tau J_\tau'}(\kappa),$$

where $S_{J_\tau J_\tau'}(\kappa)$ is the strength of the transition between the two states, κ is the molecular asymmetry parameter ($\kappa = \frac{2A-B-C}{BC}$) and μ is the molecular dipole moment. The zero field splitting Δ is obtained from the expression relating the Stark tuning rate, $d\nu/dE$, and μ_{12},

$$\frac{d\nu}{dE} = \mu_{12}\left[1 + \left(\frac{\Delta}{2\mu_{12}E}\right)^2\right]^{-1/2}$$

where E is the resonant electric field for frequency ν. For a specific choice of the state J_τ and J_τ', for the $N^{15}H_2D$ and $N^{15}HD_2$ molecules the zero field splitting between these levels can be obtained, using the measured Stark tuning rate. The zero field splittings obtained in this way may be compared with estimates of the $N^{15}H_2D$ and $N^{15}HD_2$ spectra including the rigid rotor and inversion splittings. For the observed J = 4 resonance (P(26)), a calculated zero field splitting of 1.4 GHz is obtained for the $4^a_{04} - 4^a_{14}$ levels of $N^{15}H_2D$. For the J = 6 resonance (R(18)) a zero field splitting of 10.7 GHz is obtained for the $6^a_{06} - 6^s_{16}$ levels of $N^{15}H_2D$. These levels show the closest fit to the expected rigid rotor plus inversion

energy spectrum. Substitution of N^{15} for N^{14} results in reduction of the ground state inversion frequency by $\simeq$ 500 MHz and increases the rigid rotor energy difference by $\simeq$ 70 MHz for the 4_{04} - 4_{14} states and by $\simeq$ 15 MHz for the 6_{06} - 6_{16} states. These changes result from the increase of the effective mass and the changes in (A-C)/2 and κ parameters upon substitution.[4] In this way, it is concluded that the interacting states for the P(26) and R(18) resonances are 4^a_{04} - 4^s_{14} and 6^a_{06} - 6^s_{16} of the $N^{15}H_2D$ molecule, respectively. We have also assumed that, as in $N^{14}H_2D$, Stark shifts in the upper state are negligible. The identification of the P(10) lines is complicated by the difficulty in obtaining the energy level diagram for high J transitions where centrifugal distortion effects on both rigid rotor energies and inversion frequency are large. The identification of the upper states involved in this transition awaits more detailed investigations of the microwave and infrared spectrum of the molecules, as well as more detailed calculations on the isotopic dependence of inversion splitting.

In conclusion we have found that gas mixtures of $N^{15}H_2D$ and $N^{15}HD_2$ molecules exhibit Stark tunable coincidences with the CO_2 laser on the P(28), P(26), P(10) and R(18) lines. The P(26) and R(18) are applicable to the extension of Stark cell stabilization of CO_2 lasers over as many CO_2 laser lines as possible for communications applications. From the tuning rates we identify the P(26) and R(18) resonances as being due to the $N^{15}H_2D$ molecule.

We wish to acknowledge the expert technical assistance of R. E. Brower in performing these experiments. The many helpful discussions with Dr. J. F. Lotspeich are also gratefully acknowledged.

CO_2 Laser Line	Resonance Field $\|M\| = J$ line (V/cm)	J	$\frac{d\nu}{dE}$ (MHz/V/cm)	% Absorption	Species
R(18)	4565	6	+ 0.285	> 10	$N^{15}H_2D$
P(26)	1409	4	- .432	> 10	$N^{15}H_2D$
P(10)	2952	11	- .401	≃ 2	$N^{15}H_2D$ or $N^{15}HD_2$
P(28)	2033	-	- .151	≃ 4	$N^{15}H_2D$ or $N^{15}HD_2$
P(20)	3543	4	- .564	> 10	$N^{14}H_2D$
R(12)	5397	4	+ .535	> 10	$N^{14}H_2D$
P(14)	4559	4	- .563	> 10	$N^{14}H_2D$

Table 1. Stark Resonance Parameters for $N^{15}H_2D$ and $N^{14}H_2D$ molecules. Positive μ's signify that increasing fields must be applied for increasing laser frequency. The absorption measurements are for 50:50 mixture of $N^{15}H_3$ and $N^{14}D_3$ and $N^{14}H_3$ and $N^{14}D_3$ at 1 T total pressure.

REFERENCES

1. R. L. Abrams, Appl. Phys. Lett. 25, 304 (1974).
2. T. A. Nussmeier and R. L. Abrams, Appl. Phys. Lett. 25, 617 (1974).
3. C. H. Townes and A. L. Schalow, Microwave Spectroscopy (McGraw Hill, New York, 1955), pp. 254.
4. M. T. Weiss and Strandberg, Phys. Rev. 83, 567 (1951).